Parameterization of phytoplankton spectral absorption coefficients in the Baltic Sea: general, monthly and two-component variants of approximation formulas

Justyna Meler[1], Sławomir B. Woźniak[1], Joanna Stoń-Egiert[1], Bogdan Woźniak[1†]

[1]Institute of Oceanology, Polish Academy of Sciences, Powstańców Warszawy 55, 81-712 Sopot, Poland
Correspondence to: Justyna Meler (jmeler@iopan.pl)

Abstract. The paper presents approximate formulas (empirical equations) for parameterizing the coefficient of light absorption by phytoplankton $a_{ph}(\lambda)$ in Baltic Sea surface waters. Over a thousand absorption spectra (in the 350-750 nm range), recorded during nine years of research carried out in different months of the year and in various regions of the southern and central Baltic, were used to derive these parameterizations. The empirical material was characterized by a wide range of variability: the total chlorophyll *a* concentration (*Tchla*) varied between 0.31 and 142 mg m^{-3}, the ratio of the sum of all accessory pigment concentrations to chlorophyll *a* ($\sum C_i/Tchla$) ranged between 0.21 and 1.5, and the absorption coefficients $a_{ph}(\lambda)$ at individual light wavelengths varied over almost three orders of magnitude. Different versions of the parameterization formulas were derived on the basis of these data: a one-component parameterization in the "classic" form of a power function with *Tchla* as the only variable, and a two-component formula – the product of the power and exponential functions – with *Tchla* and $\sum C_i/Tchla$ as variables. We found distinct differences between the general version of the one-component parameterization and its variants derived for individual months of the year. In contrast to the general variant of parameterization, the new two-component variant takes account of the variability of pigment composition occurring throughout the year in Baltic phytoplankton populations.

1 Introduction

If we wish to fully describe the process of photosynthesis in the seas and oceans, and to correctly interpret remote observations of water bodies, it is important to obtain an accurate quantitative description of the spectral characteristics of light absorption by living phytoplankton, a significant constituent of seawater (see e.g. Kirk 1994, Mobley 1994, or Woźniak and Dera 2007). The efficiency of sunlight absorption by this phytoplankton generally depends on a number of factors. The major, strongly absorbing components of phytoplankton cells are the pigments they contain. The principal photosynthetic pigment is chlorophyll *a*, which absorbs visible light mainly in two bands, one situated in the blue region, with a maximum around 440 nm, and another one in the red, with a maximum around 675 nm (see e.g. Bidigare et al. 1990, Bricaud et al. 2004 or Woźniak and Dera 2007). There are also various accessory pigments, like chlorophylls *b* and *c*, carotenoids and phycobilins. These latter

pigments have different spectral absorption characteristics and may be involved in photosynthetic, photoprotective or other processes in marine organisms. The pigment composition of photosynthesizing marine species can differ, since it can in a general sense reflect the adaptation of an organism to different light conditions (photo- and chromatic adaptation) as well as acclimation at the plant community level (see e.g. Kirk 1994, Woźniak and Dera 2007). Overall, analysis of pigment composition data obtained for marine phytoplankton assemblages from various ocean and sea waters has revealed a general trend indicating that the proportion of accessory pigments relative to chlorophyll *a* decreases with increasing chlorophyll *a* concentration (increasing trophicity) (see e.g. Woźniak and Ostrowska 1990, Trees et al. 2000 or Babin et al. 2003). Even so, there is substantial variability around this trend. Hence, the main factor that light absorption by phytoplankton assemblages depends on is the pigment composition. Another important factor, where absorption by phytoplankton is concerned, is how densely the strongly light-absorbing pigments are 'packed' within the internal structures of individual cells (the so-called 'packaging effect', see e.g. Morel and Bricaud 1981, 1986). Increasing intracellular pigment concentrations and cell size flatten the real absorption spectra compared to what one may expect from a simple addition of the absorption coefficients of individual pigments. Given the complexity of all these relationships, it is often necessary (or even required) for practical purposes to take a highly simplified approach, for example, when constructing models of bio-optical processes for interpreting remote sea observations. It is a common simplification to assume that all the relevant properties of a phytoplankton population can be roughly parameterized with the aid of just one variable – the concentration of chlorophyll *a*: indeed, the total biomass of an entire phytoplankton population as well as its diverse optical properties are often parameterized in this way. Earlier authors addressing this question applied this kind of simplification in attempts to determine typical values of the 'chlorophyll *a*-specific' absorption coefficient (defined as the light absorption coefficient of phytoplankton normalized to the chlorophyll *a* concentration). In practice, therefore, the adoption of one averaged value of this coefficient should enable the relationship between the phytoplankton absorption coefficient and the chlorophyll *a* concentration in seawater to be described using the simplest possible, i.e. linear, functional relationship. As measured in nature, however, values of the specific absorption coefficient have proved to be highly variable. The papers by Bricaud et al. (1995, 1998), often cited by other authors, were among the first to introduce for practical purposes a different, non-linear, approximate description of the light absorption vs chlorophyll *a* concentration relationship. They proposed using a power function to account for the general decrease in light absorption efficiency per unit chlorophyll *a* concentration that occurs with increasing absolute values of this concentration in seawater (the relevant mathematical formulas are given later in the text). Bricaud et al. (1995) also gave a theoretical explanation of these effects, suggesting that there might be a correlation between the increase in the absolute chlorophyll *a* concentration and the increasing contribution of the pigment packaging effect and, concurrently, the decreasing proportion of pigments other than chlorophyll *a*. The papers by Bricaud et al. (1995, 1998) were based on extensive empirical material gathered in different regions of open, oceanic waters, classified as 'case 1 waters'. Different authors addressed the same problem in many later papers: examples of spectral power function parameterizations for different marine environments can be found in, for example, Stramska et al. (2003), Staehr and Markager (2004), Matsuoka et al. (2007), Dmitriev et al. (2009), Nima et al. (2016), Churilova et al. (2017) and Mascarenhas et al. (2018). The subject literature also provides examples of similar

parameterizations derived for inland water bodies, for example, by Reinart et al. (2004), Ficek et al. (2012a, b), Ylöstalo et al. (2014) and Paavel et al. (2016). All of these papers give spectral coefficients of parameterizations tailored to specific datasets differing from each other to a greater or lesser extent. Obviously, all such parameterizations are far-reaching simplifications of the complex dependences observed in nature. That there might be significant deviations from the approximate "average"

5   relationship was already made clear by Bricaud et al. (1995) in their original work; these authors subsequently analysed the potential causes of this differentiation (Bricaud et al. 2004). Using indirectly reconstructed information regarding the size structure of the ocean phytoplankton population, they were able to estimate separately the impacts of the differences in the dominant sizes of plankton populations and the differences in pigment composition on the relationship in question. In general, they found that for oligo- and mesotrophic waters (i.e. waters with chlorophyll a concentrations < 2 mg m^{-3}), the variability

10 associated with the packaging effect might be exerting a more significant influence, whereas in eutrophic waters (with higher chlorophyll a concentrations) both effects might be of equal weight. Generally, however, the observed variability indicates that one should expect both regionally and seasonally differentiated forms of such simplified relationships to occur instead of one universal, approximate statistical relationship between $a_{ph}(\lambda)$ and the chlorophyll a concentration.

The Baltic Sea, the region we have been studying, is a semi-enclosed, brackish water basin classified as an example

15 of 'case 2 waters'. It is characterized by usually high concentrations of terrigenous dissolved organic substances (see e.g. Kowalczuk 1999). The biomass and species composition of living phytoplankton in the Baltic is known to vary during the year. Usually there are three main phytoplankton blooms: a spring bloom of cryophilous diatoms, which transforms into a bloom of dinoflagellates (early March – May), a summer bloom of cyanobacteria (July and August), and an autumn bloom of thermophilous diatoms (September – October) (see Wasmund et al. 1996 and 2001, Witek and Pliński 1998, Wasmund and

20 Uhlig, 2003, Thamm et al. 2004).

In an earlier paper by our research team (Meler et al. 2017a) we provided an initial version of the power function parameterization, adjusted to data collected in the southern Baltic Sea. However, these preliminary analyses, focusing mainly on pooled data from marine and lacustrine environments, were based on a much smaller set of data than the one we currently have, and the initial parameterization was carried out for all the data pooled, regardless of when they were acquired. On the

25 other hand, another recent paper of ours identified significant differences in the absorption properties of Baltic phytoplankton at different times of the year (Meler et al. 2016b). In a further preliminary study, limited to just the single light wavelength of 440 nm, we demonstrated differences between the coefficients of the relevant simplified parameterizations when they were tailored to data gathered at specific times of the year (Meler et al. 2017b). It is in this context, therefore, that we have decided in the present paper to re-address the problem of determining practical forms of a simplified parameterization of the

30 phytoplankton absorption coefficient appropriate to Baltic Sea conditions.

The objectives of this work are twofold:

- the main one is to find new forms of the classic, one-component power function parameterization for the phytoplankton absorption coefficient adapted to the specific conditions of the Baltic Sea. An important aspect of this is to record the extent of the differences between the coefficients of spectral parameterization when they are derived separately for data from selected

periods of the year. These new analyses, as opposed to the preliminary results published earlier, have to be performed over a wide spectral range, with a sufficiently high resolution, on the currently available extended dataset and also in accordance with the latest recommended calculation procedures;

- an additional aim of this work is to propose a modified, but still relatively simple, new form of parameterization enabling the diversity of phytoplankton absorption properties observed in the study area during the year to be taken into account.

The new forms of parameterization that we are seeking can be used, among other things, to develop and improve the accuracy of practical, local algorithms for interpreting remote observations of the Baltic Sea.

2 Materials and methods

The empirical data used in this study were collected at more than 170 measuring stations in various parts of the southern and central Baltic Sea, though mainly in the Polish economic zone, from 2006 to 2014 (see Figure 1). These data were acquired principally during 42 short research cruises on board r/v Oceania at different times of the year, but mostly from March to May and from September to October (about 80% of the data analysed in this paper are from these periods). The practice during each cruise was to select measuring stations that were maximally diverse with respect to their optical properties, i.e. in the vicinity of river mouths and estuaries (the Rivers Vistula, Oder, Reda, Łeba and Świna; the Szczecin Lagoon), bays and offshore waters (Gulf of Gdańsk, Puck Bay and Pomeranian Bay), and open southern Baltic waters. During three cruises (in May of 2010, 2012 and 2014), measurements were also made in the open waters of the central Baltic. However, because of weather- and sea-state-related limitations, only 32% of the data are from open water regions (see Table 1). In addition to the cruise measurements, data were gathered throughout the year by sampling the seawater at the end of the ca 400 m long pier in Sopot, on the Gulf of Gdansk coast (< 7% of the overall number of data analysed).
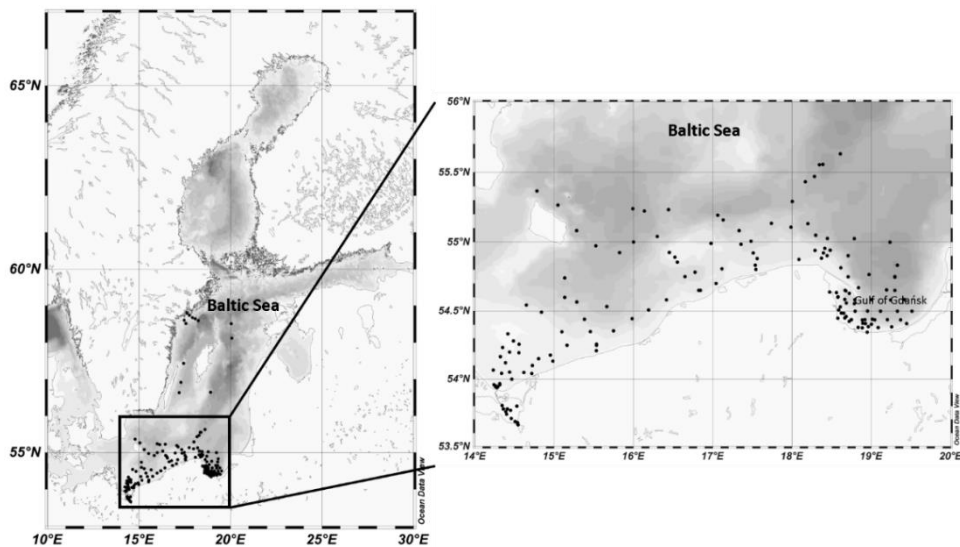

Figure 1. Locations of all the sampling stations in the Baltic Sea; enlarged view of the study area.

Table 1. Numbers of seawater samples analysed, divided into the months and areas of their acquisition.

Time of the year	Open Baltic Sea areas	Coastal areas and bays	All regions
January	4	6	10
February	16	36	52
March	52	122	174
April	22	74	96
May	80	121	201
June	-	5	5
July	-	7	7
August	4	21	25
September	75	136	211
October	51	101	152
November	15	42	57
December	1	11	12
All year	320	682	1002

During the research cruises, a diversity of physical and optical parameters of seawater were measured *in situ* at each sampling station, and discrete seawater samples were collected for further laboratory analysis of certain optical properties (spectra of coefficients of light absorption by phytoplankton) and biogeochemical properties (concentrations of chlorophyll *a* and other phytoplankton pigments). These samples were collected with a Niskin bottle (height ca 0.9 m, capacity 25L) immersed just below the surface; in shallow estuarine areas and river mouths (sampled from a pontoon) or off the end of the Sopot pier, they were obtained with a bucket. Immediately after collection, all samples were passed through glass fibre filters (Whatman, GF/F, 25 mm, nominal retention of particles with sizes down to 0.7 μm) at a pressure not exceeding 0.4 atm. The volumes filtered were chosen on a case-by-case basis; between 2 and 1150 ml of seawater were filtered for later absorption measurements, and generally between 150 and 1000 ml for phytoplankton pigment concentration analysis). All sample filters were immersed in a Dewar flask containing liquid nitrogen (at about -196°C) and then kept frozen (at about -80°C) for further analysis in the laboratory on land.

In order to determine the spectra of the phytoplankton absorption coefficient a_{ph}, we measured the absorption coefficient spectra for all suspended particles retained on filters (a_p), and also, after chemical bleaching of the pigments in our samples, the corresponding spectra of non-algal particles (a_{NAP}). We performed the optical measurements in the 350-750 nm spectral range with a UNICAM UV4-100 double-beam spectrophotometer equipped with an integrating sphere of external diameter 66 mm (LABSPHERE RSA-UC-40). For the reference measurements we used clean filters rinsed with particle-free seawater. The methodology of combined light-transmission and light-reflection measurements (known as the T-R method) was that described by Tassan and Ferrari (1995, 2002). From the pooled results of these measurements (several scans in

different configurations), we calculated the optical density $OD_s(\lambda)$ representing each filtered sample. As opposed to standard spectrophotometric analyses performed in transmission mode only, at least in theory, the results of T-R method should not need to be corrected for the so-called 'scattering error'. But in order to calculate absorption coefficients of particles in solution, an additional correction has to be made to compensate for the elongation of the optical path of the light owing to the multiple scattering occurring in the filtered material. This is done by applying the dimensionless path length amplification, the β-factor, which converts the measured optical density of particles collected on the filter ($OD_s(\lambda)$) into the optical density characterizing these particles in solution ($OD_{sus}(\lambda)$) (Mitchell 1990). In our analyses we used the new β-factor formula proposed by Stramski et al. (2015) for the T-R method:

$$OD_{sus}(\lambda) = 0.719 OD_s(\lambda)^{1.2287}. \tag{1}$$

The coefficient of light absorption by all suspended particles was then calculated using the formula:

$$a_p(\lambda) = [\ln(10) \cdot OD_{sus}(\lambda)]/l, \tag{2}$$

where l [m] is the hypothetical optical path in solution, determined as the ratio of the volume of filtered water to the effective area of the filter. The absorption by non-algal particles $a_{NAP}(\lambda)$ was determined in an analogous way, after the phytoplankton pigments had been bleached for 2-3 minutes with a 2% solution of calcium hypochlorite $Ca(ClO)_2$ (Koblentz-Mishke et al. 1995, Woźniak et al. 1999); thereafter the sample filter was rinsed with a small volume of particle-free seawater to remove any bleach residue, as this could additionally absorb light at short wavelengths. Finally the sought-after coefficient a_{ph} was calculated as the difference between a_p and a_{NAP}.

In practice, however, we had to add two corrective procedures to the protocols described above. One related to the noise which appeared in the individual spectra recorded with our spectrophotometer. To partially eliminate it, we applied a 'spectral smoothing' procedure – the spectral 5-point 'moving average' was repeated 3 times – to the calculated individual spectra of both coefficients a_p and a_{NAP}. This procedure partially eliminated fluctuations of the signal between adjacent light wavelengths but did not significantly affect the magnitude of the major absorption peaks, the 'half-widths' of which are of the order of tens of nm. The other corrective procedure related to the small deviations from zero of the calculated coefficients a_{ph} at wavelengths close to 750 nm. It is generally assumed that the light absorption of phytoplankton pigments in this spectral range should be negligible (Babin and Stramski, 2002). The occurrence of non-zero values in this range may be due to several different factors: differences in the optical properties of individual glass fiber filters, the difficulty of maintaining ideally repeatable filter moisture during measurements, and the possible partial loss of sample material as a result of the filters being rinsed after bleaching. To correct for all these effects we applied a simple 'null-point' correction (see e.g. Mitchell et al. 2002). The average coefficient a_{ph} calculated in the range between 740 and 750 nm was subtracted from the values of a_{ph} across the entire spectrum. Generally different factors may have influenced the final uncertainty of our absorption measurements. Among them is the instrument noise present in each individual spectrophotometric scan (in each configuration), and also the possible uncertainty in path length amplification factor, volume filtered and filter area used in subsequent calculations, as well as

uncertainty coming from subsampling from larger volumes of water. As a strict estimation of all these inaccuracies would be very complicated (due to the mathematical complexity of the algorithm used according to Tassan and Ferrari (1995, 2002)), here we limit ourselves only to estimating some of these inaccuracies. The mean inaccuracy caused by instrument noise occurring in separate measurements of light absorption by particles before and after bleaching we estimated to be $\Delta a_{ph} =$ 5.68*10^{-3} m^{-1} (± 9.13*10^{-3} m^{-1}, standard deviation (SD)). We assumed that the uncertainty of a_{ph} (Δa_{ph}) can be calculated as a square root of a sum of squares of uncertainties Δa_p and Δa_{NAP} . The latter were estimated as 95% prediction intervals (=1.96 SD) for a_p and a_{NAP} values between 740 and 750 nm, where it is assumed that the absorption signal should be flat. Dividing the mean value of Δa_{ph} by corresponding measured values of $a_{ph}(440)$ or $a_{ph}(675)$ gave percentage error distributions with mean values of 2.3% and 5.9%, respectively (with SD of 2.3% and 7.6%, respectively). In the collected data set, due to logistic limitations, generally no measurements were made on multiple samples. However, in the separate tests we estimated the average uncertainty of a_{ph} measurements due to subsampling to be 9.1% (± 1.5%, SD).

HPLC was used to determine phytoplankton pigment concentrations; the methodology is described in detail in Meler et al. (2017b), Stoń and Kosakowska (2002) and Stoń-Egiert and Kosakowska (2005). In this work we refer mainly to the total chlorophyll a concentration ($Tchla$) (defined as the sum of chlorophyll a, allomer and epimer, chlorophyllide a and phaeophytin a), and to the sum of the concentrations of all accessory pigments ΣC_i, i.e. the sum of chlorophylls b ($Tchlb$), chlorophylls c ($Tchlc$), photosynthetic carotenoids (PSC) and photoprotective carotenoids (PPC). The precision of HPLC measurements was estimated as equal to 2.9% (±1.5%, SD), and an error related to subsampling as 9.7% (±6.4%, SD) (Stoń-Egiert et al., 2010).

The data were analysed statistically in order to characterize their variability and to find approximate empirical relationships between them. The variability of the target optical and biogeochemical quantities ranged over almost three orders of magnitude. Therefore, to assess the uncertainty of our empirical parameterizations, we applied standard arithmetic statistics of relative error, and also separate statistics of logarithmically transformed data (so-called logarithmic statistics). The exact formulas are given as a footnote to one of the tables later in the paper.

3 Results and discussion

3.1 General characteristics of the data

Figure 2 exemplifies selected spectra of a_{ph} that we recorded in the Baltic Sea. Even though they were smoothed using the previously described raw data procedure, some still contain artefacts related to the noise occurring in our measurement system. These artefacts are particularly visible in the 350-400 nm range, where the accuracy of measurements is limited owing to the strong light attenuation by the glass fibre from which the filters are made, and also in the 550-650 nm range, where the absorption signal is small compared to other bands. In spite of these imperfections, 80% of these spectra exhibit the expected characteristic absorption maxima in both the blue (ca 440 nm) and red (ca 675 nm) bands. Some of the spectra in our set, however, do not show a significant increase in light absorption with increasing wavelength in the 350-440 nm range: in 20% of the spectra recorded $a_{ph}(400)/a_{ph}(440)$ is > 0.95 (in some cases as high as 1.42), mainly for samples from near the mouth of

the River Vistula, in the Szczecin Lagoon and off the Sopot pier. The first part of Table 2 lists basic statistical information characterizing the ranges of variation of the light absorption coefficient at selected light wavelengths. In fact, the variability of $a_{ph}(\lambda)$ over the entire spectral range examined, calculated for individual light wavelengths, was almost three orders of magnitude. For blue light, for example, $a_{ph}(440)$ varied from 0.014 m^{-1} to 3.85 m^{-1}, whereas for the local absorption maximum in the red band, $a_{ph}(675)$ varied from 0.006 m^{-1} to 1.74 m^{-1}.
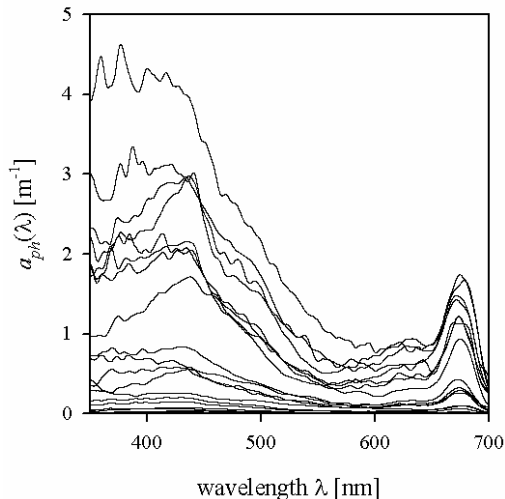

Figure 2. Examples of spectra of the light absorption coefficient $a_{ph}(\lambda)$ representing the variability range of the data analysed in the present paper.

Table 2. Variability ranges of selected optical and biochemical quantities characterizing phytoplankton in samples from the Baltic Sea.

Quantity	Average value (CV)	Minimum; 10th perc.;**median**; 90th perc.; maximum
$a_{ph}(350)$ [m^{-1}]	0.222 (166%)	0.007; 0.033; **0.103**; 0.509; 3.91
$a_{ph}(440)$ [m^{-1}]	0.280 (137%)	0.014; 0.059; **0.157**; 0.611; 3.85
$a_{ph}(500)$ [m^{-1}]	0.142 (142%)	0.007; 0.029; **0.080**; 0.313; 2.17
$a_{ph}(550)$ [m^{-1}]	0.065 (145%)	0.003; 0.012; **0.036**; 0.147; 1.17
$a_{ph}(600)$ [m^{-1}]	0.044 (166%)	0.002; 0.007; **0.021**; 0.093; 0.772
$a_{ph}(675)$ [m^{-1}]	0.133 (148%)	0.006; 0.023; **0.069**; 0.290; 1.74
$a_{ph}(700)$ [m^{-1}]	0.022 (180%)	0.0001; 0.003; **0.010**; 0.049; 0.459
$Tchla$ [mg m^{-3}]	7.69 (163%)	0.31; 1.09; **3.63**; 17.92;141.8
$Tchlb$ [mg m^{-3}]	0.50 (175%)	0; 0.07; **0.27**; 1.01; 11.7
$Tchlc$ [mg m^{-3}]	0.76 (149%)	0.01; 0.09; **0.35**; 1.93; 14.8
PSC [mg m^{-3}]	1.82 (175%)	0.03; 0.15; **0.73**; 4.52; 32.1
PPC [mg m^{-3}]	1.70 (160%)	0.04; 0.26; **0.86**; 3.89; 42.8
ΣC_i[mg m^{-3}]	4.79 (152%)	0.15; 0.69; **2.40**; 6.02; 72.1
$\Sigma C_i\,/\,Tchla$	0.66 (27%)	0.21; 0.47; **0.62**; 0.88; 1.50

The second part of Table 2 provides statistical information illustrating the variability in concentration of the basic photosynthetic pigment chlorophyll *a* (*Tchla*), and also the concentrations of different groups of accessory pigments, i.e. chlorophylls *b* and *c*, and other photosynthetic and photoprotective pigments (*Tchlb, Tchlc*, *PSC* and *PPC*). In addition, the table lists the total concentration of all accessory pigments (ΣC_i) and the $\Sigma C_i/Tchla$ ratio. Figure 3 illustrates the variabilities of *Tchla* and ΣC_i as well as their ratio for all the pooled data, broken down into individual sampling periods (months). This shows that with respect to all the data analysed, the ranges of variability of both *Tchla* and ΣC_i are, like the absorption coefficient, almost three orders of magnitude (0.41-141.8 mg m^{-3} and 0.15-72.1 mg m^{-3} respectively). The average *Tchla* for all the data was 7.69 mg m^{-3}. In the spring and summer months when we were able to make measurements at sea, mean values of *Tchla* were above average, while in autumn and winter they were lower. In general, a similar trend of average changes in individual months emerges from an analysis of the sum of accessory pigment concentrations ΣC_i. Taking into account all the data from different periods of the year, we can say that measured values of ΣC_i correlate fairly well with *Tchla* (see the approximate equation and the coefficient of determination R^2 given in Figure 3c). Nevertheless, if we look at the $\Sigma C_i/Tchla$ ratio, we see that its average values also changed significantly during the year (see Figure 3b). The average $\Sigma C_i/Tchla$ for all the data was 0.66, but the full range of variability that we recorded was from 0.21 to 1.5. For the months of April, May and September, the average $\Sigma C_i/Tchla$ was higher than or equal to the average for the whole year (0.66, 0.79 and 0.69, respectively). In the remaining months, the averages were lower than the general average – from 0.50 to 0.61. This latter fact is a clear indicator of the obvious limitations of applying solely the chlorophyll *a* concentration as a simplified measure to describe the overall pigment population, and to which measure the light absorption of pigments is customarily parameterized.
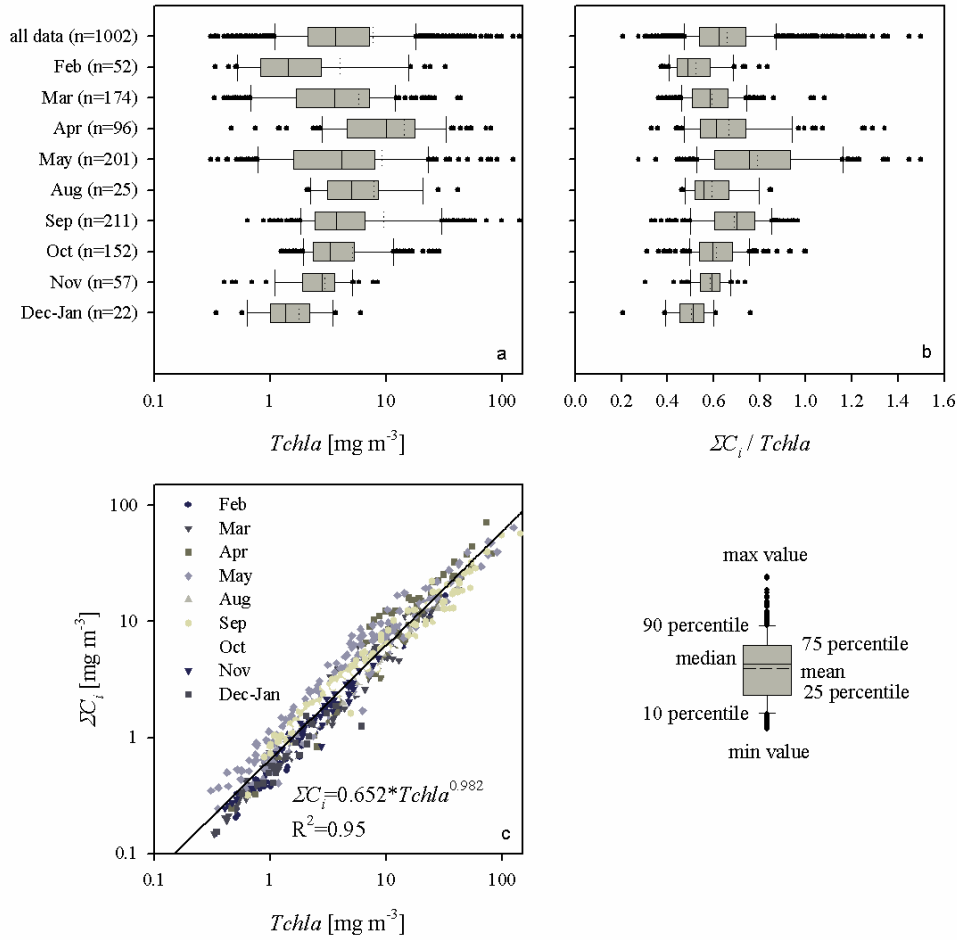
Figure 3. (a): Box plot presenting the range of variation of chlorophyll *a* concentration (*Tchla*) for all the data analysed and for each sampling month; (b): as (a) but showing the ratio of the sum of accessory pigments to the chlorophyll *a* concentration ($\Sigma C_i/Tchla$); (c): graph illustrating the relationship between ΣC_i and *Tchla* – the solid line represents a simple functional approximation of the relationship (the equation is given in the panel).

3.2 Approximate description of the light absorption coefficient by phytoplankton

3.2.1 General and monthly variants of one-component parameterizations

We carried out statistical analyses of our measurement data in order to define classic forms of the approximate functional relations between the light absorption coefficient $a_{ph}(\lambda)$ and the concentration *Tchla*. Like Bricaud et al. (1995, 1998), we approximated these relations using power functions. With linear regression applied to the logarithms of the input data for each light wavelength (regression between $\log(a_{ph}(\lambda))$ and $\log(Tchla)$), the coefficients *A* and *E* of the following approximated parameterization could be calculated:

$$a_{ph}(\lambda) = A(\lambda) \cdot Tchla^{E(\lambda)}, \tag{3.a}$$

Note that coefficient $A(\lambda)$ determined in this way reflects the numerical value of the light absorption coefficient $a_{ph}(\lambda)$ that the approximated relationship assigns to the case when the *Tchla* is exactly 1 mg m^{-3}. The coefficient $E(\lambda)$ of equation (3.a) is a dimensionless quantity, which is the exponent of the power to which the chlorophyll *a* concentration is raised. If its value is

5   <1, there is a statistical tendency for the phytoplankton absorption efficiency to decrease per unit mass of chlorophyll *a* with increasing absolute chlorophyll *a* concentration. A value of $E=1$ would mean a stable a_{ph} to *Tchla* ratio, while a value of $E>1$ would imply a statistical tendency for a_{ph}/*Tchla* to increase with increasing *Tchla*. By performing linear regression of the logarithms of the input data, we were also able to calculate the determination coefficients R^2 for the approximated parameterization at the individual wavelengths of light. The parameterization coefficients *A* and *E* given by formula (3.a) can

10   be easily used to determine the specific coefficient of light absorption by phytoplankton $a_{ph}^*(\lambda)$ [m^{2}mg^{-1}] (defined as values of $a_{ph}(\lambda)$ normalized with respect to *Tchla*):

$$a_{ph}^*(\lambda) = A(\lambda) \cdot Tchla^{E(\lambda)-1}. \tag{3.b}$$

The coefficients of the approximate formula (3.a) were determined over the entire available spectral range from 350 to 700 nm with a resolution of 1 nm. Figures 4a, b and c present different variants of the spectra of coefficients $A(\lambda)$ and $E(\lambda)$,

15   along with the respective values of R^2. These variants represent parameterizations based on all available data (a general variant) as well as alternative parameterizations derived for data subsets relating to particular months (monthly variants). The parameterization coefficients for the general and selected monthly variants are listed in the Appendix 1 (see Tables A1 and A2). Analysis of the curves in Figures 4a and b shows that the coefficients of the monthly parameterizations differ, exhibiting larger or smaller deviations from the course of the general variant's coefficients. In the case of coefficient *A*, the differences

20   between 350-590 nm and around 675 nm are particularly conspicuous. For example, the highest values of coefficient *A* for the 440 nm band were obtained in the case of parameterizations derived for September and December-January, and the lowest for April. With regard to the spectral slope of coefficient *A* in the 350-440 nm range, the largest deviations from the typical course were recorded for December-January, April, and February. In contrast, the parameterizations obtained for March, May and October are the closest to the general variant with respect to *A*. As regards coefficient *E*, there are differences between the

25   alternative parameterizations over the entire spectral range. In the general variant, *E* changes only slightly, between 0.81 and 0.91. On the other hand, the values of *E* for the parameterizations derived for individual months are spectrally more differentiated, with more pronounced local maxima and minima. The deviations from the general case of the parameterizations are the largest for March and April (upward) and for December-January (downward). The determination coefficients R^2, which may initially characterize the accuracy of the absorption coefficient parameterization using formula (3.a), are relatively high

30   in the case of general variant of parameterization, i.e. no less than 0.8, over almost the entire visible light range. Lower values of R^2 are found only at the edges of the spectral range examined, where either the accuracy of measurements is expected to be lower (short wavelengths), or the values of the absorption coefficient are close to zero (long wavelengths). In the case of the

monthly parameterizations, only the formulas obtained for months with relatively large amounts of data take equally high values of R^2 (i.e. March, April, May and September). For the other months, values of R^2 are <0.8, at least in significant parts of the spectral range examined.
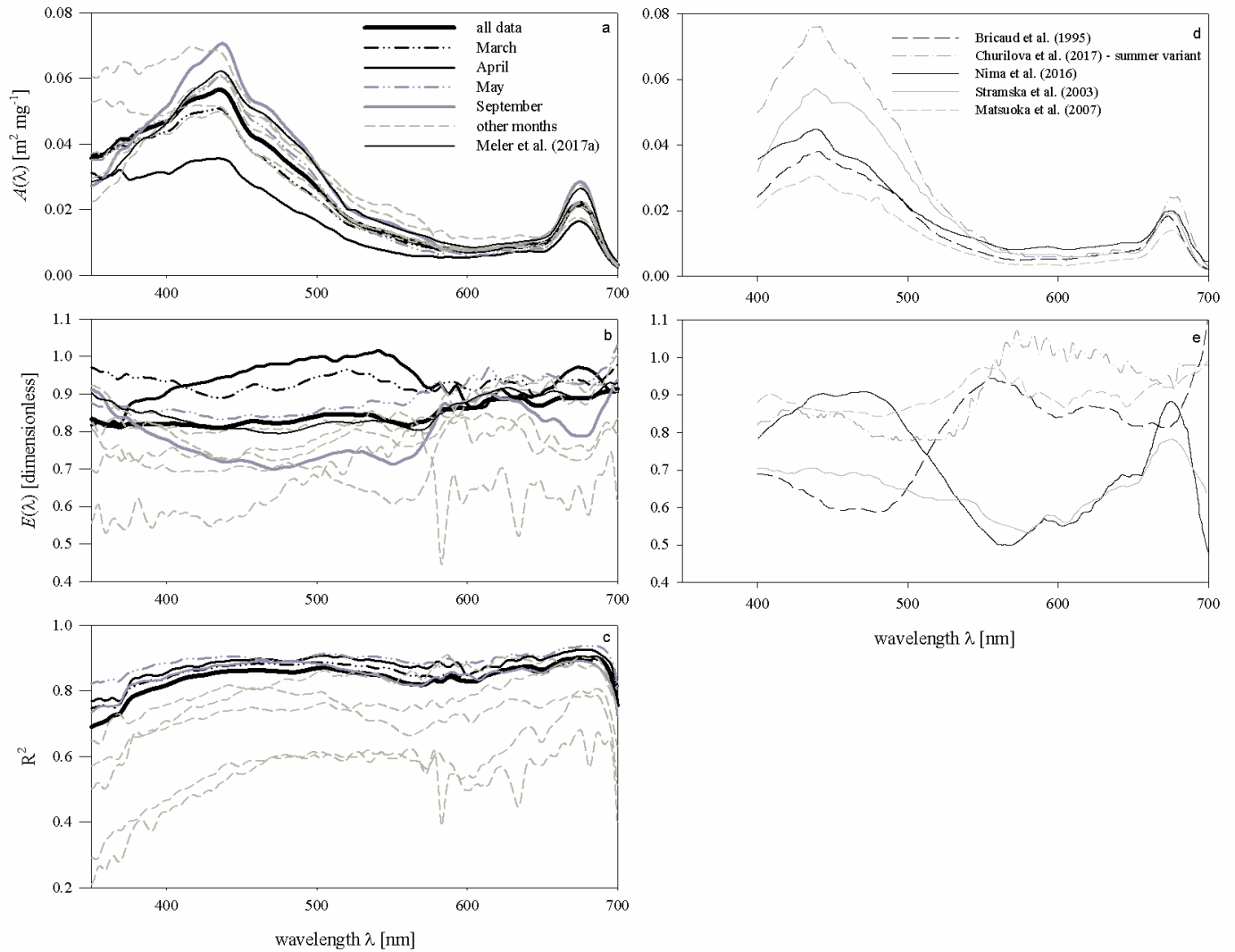
Figure 4. (a) and (b): Spectral plots of coefficients A and E of the parameterizations described by Eq. (3.a), and (c): the corresponding values of coefficient R^2, determined for all the data analysed and for each sampling month. The coefficients of the preliminary parameterization given in Meler et al. (2017a) are also plotted; (e) and (f) examples of coefficients A and E given by various authors (see the legend in panel (e)).

Figure 5 illustrates important aspects of the variability in magnitude and spectral shape of the absorption coefficient when certain variants of the parameterization are used to calculate it. Figure 5a illustrates the family of curves representing the specific coefficients of light absorption by phytoplankton $a_{ph}^*(\lambda)$ calculated according to the general variant of our new

12

parameterization. These curves are plotted for a few chlorophyll *a* concentrations from the 0.3-100 mg m^{-3} range (corresponding more or less to the range that we recorded in the Baltic Sea). The bold line in Figure 5a outlines the spectrum calculated for *Tchla* = 1 mg m^{-3} (corresponding to the numerical value of coefficient $A(\lambda)$). In addition, to better visualize the 'evolution' of the spectral shape of the predicted spectra of a_{ph}, another family of curves is plotted. The spectra of a_{ph},

5   normalized with respect to 440 nm, are plotted in Figures 5b and f for values of *Tchla* from the same range. To provide some background, Figures 5c and d show two analogous diagrams obtained using the 'classic' parameterization developed by Bricaud et al. (1995) (although it should be mentioned that the two highest *Tchla* values – 30 and 100 mg m^{-3} – generally lie beyond the range for which Bricaud et al. (1995) originally developed their parameterization). Both parameterizations, our new one and the 'classic' one according to Bricaud et al. (1995), clearly predict drops in $a_{ph}^{*}(\lambda)$ with increasing *Tchla*. But

10   where changes in spectral shapes are concerned, our general parameterization predicts significant changes only in the 600-680 nm spectral range, whereas according to Bricaud et al. (1995) the variations should occur over a much broader spectral range (see Figures 5 b and d). Both parameterizations qualitatively predict the well-known phenomenon of absorption spectra 'flattening' with increasing *Tchla* (see e.g. Morel and Bricaud 1981), but these predictions are quantitatively different. As a simplified measure of spectra 'flattening', one can analyse, for example, the changes in the ratio of $a_{ph}(440)$ to $a_{ph}(675)$: this

15   ratio is sometimes referred to as the 'colour' or 'pigment' index (see e.g. Woźniak and Ostrowska 1990 a and b; see also Bricaud et al. 1995). When the parameterization by Bricaud et al. (1995) is applied to the range of *Tchla* changes assumed here (from 0.3 to 100 mg m^{-3}), the colour index changes roughly threefold, i.e. it decreases from 2.69 to 0.88, the latter value signifying a greater absorption of light in the red band than in the blue. By contrast, with our new parameterization, the colour index drops by a factor of only around 1.57 (from 2.76 to 1.76). These differences indicate that the combined influence of the

20   packaging effect and the decrease in relative accessory pigment concentrations manifests itself differently in our Baltic Sea dataset than in the original oceanic dataset of Bricaud et al. (1995). Besides these differences, however, we would also like to point out clear differences that become apparent when different parameterizations matched to individual months are applied to our dataset. The next four panels in Figure 5 (e, f, g and h) show similar spectral curves for two contrasting months: April and September. The family of $a_{ph}^{*}(\lambda)$ curves plotted for April (Figure 5e) shows generally much lower values in the blue light

25   maximum, and less steep slopes around this maximum than the corresponding curves for September (Figure 5g). Also, the variability in the normalized shapes of coefficient a_{ph} is greater and more complex for these two particular months (Figures 5f to h) than was the case with the general parameterization (Figure 5b). The colour index changes only by a factor of 1.16 (a drop from 2.2 to 1.9) for April, while for September the corresponding change is by a factor of 1.49 (a drop from 2.7 to 1.8). There are, moreover, differences in the 'evolution' of slopes in the short-wave part of the spectrum between these two months

30   that were not manifested by the general version of our parameterization.
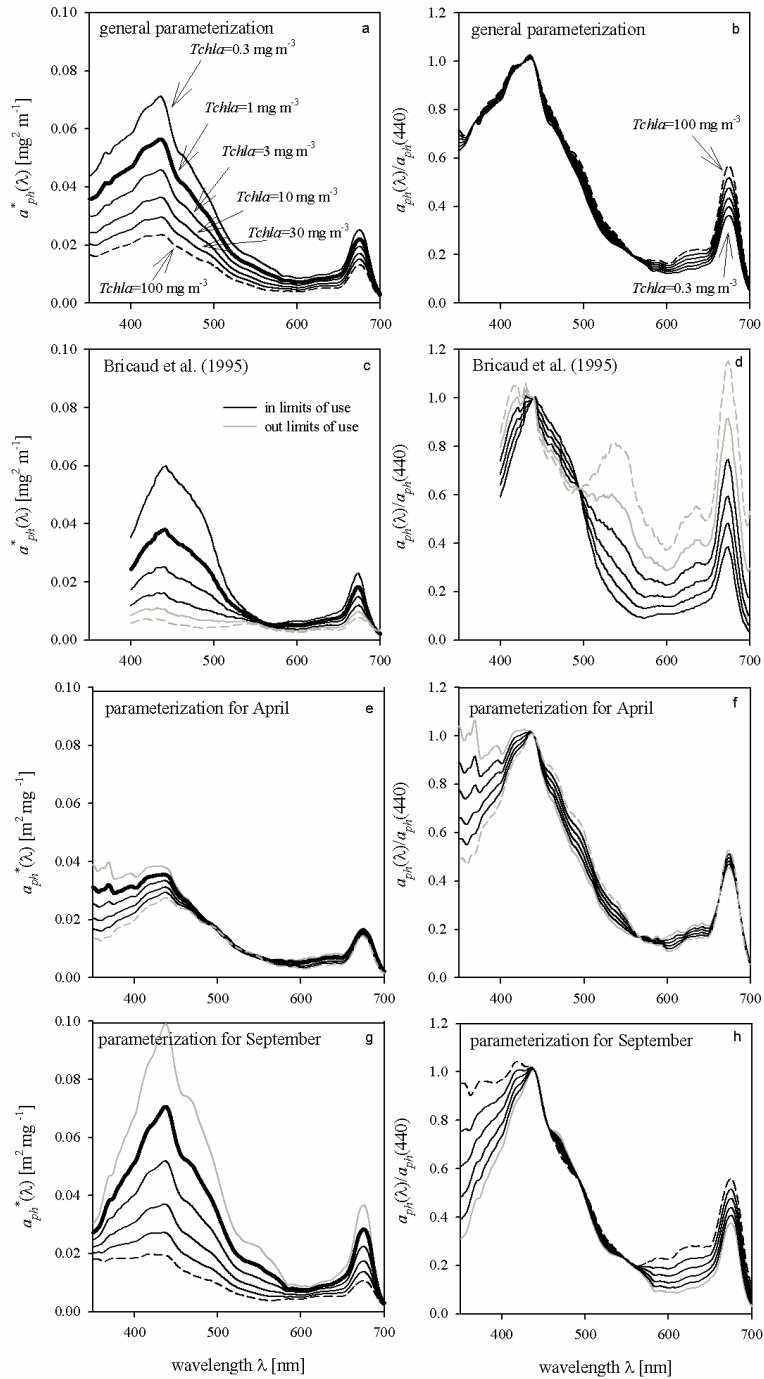
Figure 5. Example spectra of the specific coefficients of light absorption by phytoplankton $a^*_{ph}(\lambda)$ (left-hand panels) and spectra of a_{ph} normalized to its own value in the 440 nm band (right-hand panels) for some values of *Tchla* between 0.3 and 100 mg m^{-3}: (a) and (b): estimated using the general variant of the parameterization obtained in this paper; (c) and (d): estimated on the basis of the parameterization by Bricaud et al. (1995) (the grey lines on panels (c) and (d) represent chlorophyll *a*

concentrations $Tchla$ that go beyond the range for which the Bricaud et al. parameterization was originally developed); (e) and (f): estimated using the variant of parameterization obtained in this paper for April data only; (g) and (h): estimated using the variant for September data only.

Distinct differences between different months can also be visualized by plotting the mass-specific absorption coefficients a_{ph}^* at selected bands against chlorophyll a concentrations. Figures 6a and 6b illustrate such plots for 440 and 675 nm bands. Evident differences in the slopes of approximate curves for the selected four months can be seen. Although for May and March we obtain slopes of the a_{ph}^* vs $Tchla$ relationships relatively close to those obtained for the whole dataset, quite different values are obtained for April and September.
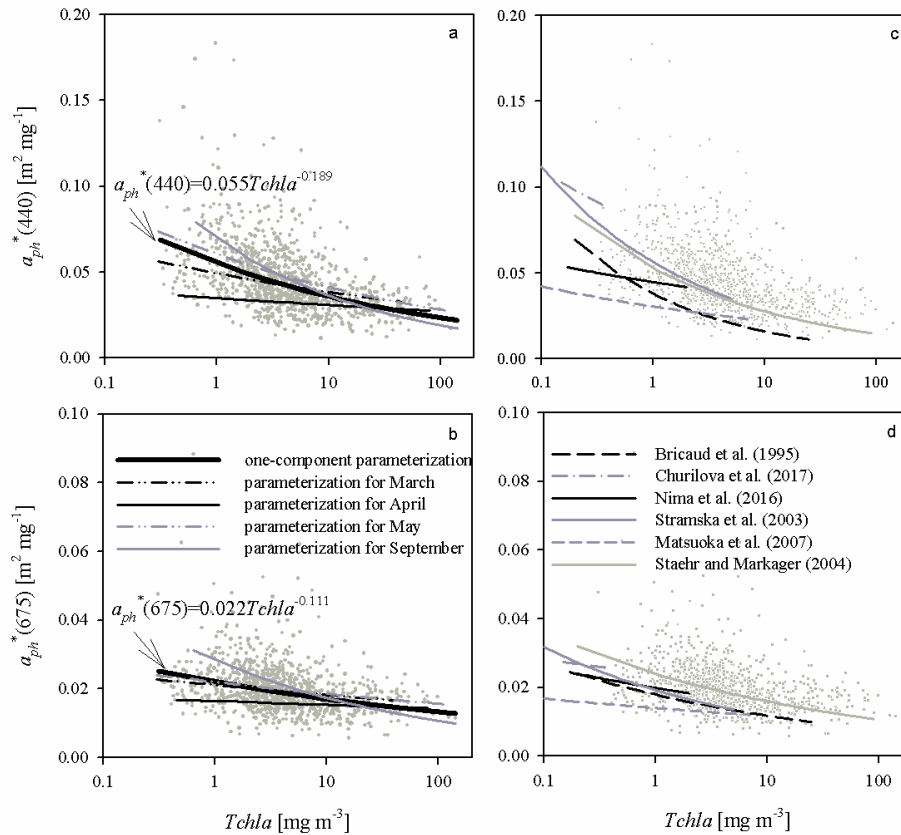
Figure 6. (a): Relationship between coefficient $a_{ph}^*(440)$ and the chlorophyll a concentration $Tchla$ and its functional approximations determined in this study for all the data analysed and for selected sampling months (see the legend to panel b; the equation given in the panel represents approximations of all the data available; for coefficients obtained for particular months, see Table A2 in Appendix 1); (b): as (a) but for $a_{ph}^*(675)$; (c) and (d) plots similar to (a) and (b) but presenting examples of functional approximations determined by various authors (see the legend to panel d). The grey dots on each panel represent individual data points from our database.

3.2.2 Two-component parameterization

As already indicated in section 3.1, there is a noticeable variation in the proportion between *Tchla* and the concentrations of other phytoplankton pigments in particular months of the year within our dataset (Figure 3). This variability initially indicated the limitations that may crop up when the chlorophyll *a* concentration is used as the only variable for parameterizing the spectra of $a_{ph}(\lambda)$. Such limitations became clear when we recorded the differences between the parameterizations matched to the data from selected months. As a step towards improving the accuracy of a_{ph} parameterization, while retaining the relative simplicity of the mathematical formalism used, we decided to search for one additional variable. Different candidates for this variable were tested: various ratios between concentrations of different groups of accessory pigment concentrations (*Tchlb*, *Tchlc*, *PSC*, *PSP*, their partial sums, and the sum *ΣCi*) and *Tchla*. As a result of these tests we found that the best for this particular purpose was the ratio of all accessory pigments to chlorophyll *a* (*ΣCi/Tchla*). The new expression that approximates $a_{ph}(\lambda)$ by treating it as a function of two variables at each light wavelength can be written as follows (more details on how the new formula was derived are given in Appendix 2):

$$a_{ph}(\lambda) = A_0(\lambda) \cdot e^{K(\lambda) \cdot \frac{\sum C_i}{Tchla}} \cdot Tchla^{E(\lambda)}. \tag{4}$$

The numerical coefficients of the new parameterization, i.e. $A_0(\lambda)$ [$m^2\,mg^{-1}$] and $K(\lambda)$ [no units], are summarized in Table A3 in Appendix 1 (with a spectral resolution of 2 nm). Note that coefficient $E(\lambda)$ [no units] takes the same values as those in the general variant of the one-component parameterization. Note, too, that the product of the new coefficient $A_0(\lambda)$ and the exponential function appearing in equation (4) allows one, with the adopted value of the ratio *ΣCi/Tchla*, to calculate the value corresponding to coefficient $A(\lambda)$ from the parameterization given by formula (3.a). We define this product as:

$$A'\left(\lambda, \frac{\sum C_i}{Tchla}\right) = A_0(\lambda) \cdot e^{K(\lambda) \cdot \frac{\sum C_i}{Tchla}}. \tag{5}$$

Spectral values of the new coefficients of equation (4) (coefficients $A_0(\lambda)$ and $K(\lambda)$) are shown in Figure 7.a, and Figure 7.b illustrates the family of $A'(\lambda, \Sigma C_i/Tchla)$ curves plotted for some values of *ΣCi/Tchla* in our database.

16
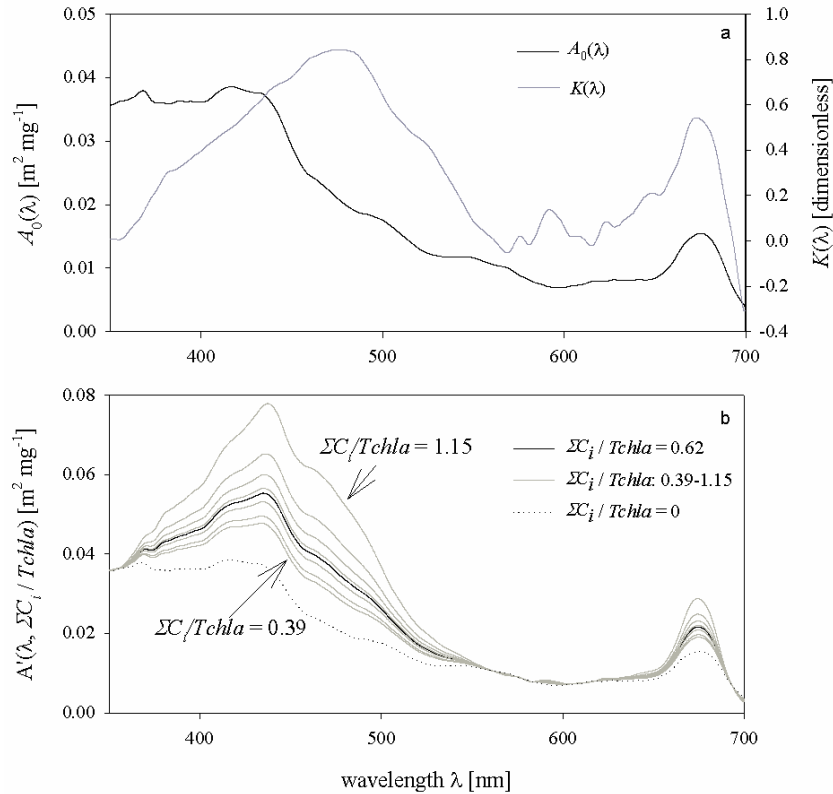
Figure 7. (a): Spectral plots of coefficients A_0 and K of the two-component parameterization described by Eq (4); (b): examples of curves representing coefficient $A'(\lambda, \Sigma C_i/Tchla)$, defined by Eq. (5), for the following values of $\Sigma C_i/Tchla$: the average value of 0.62; selected values between 0.39 and 1.15 (representing the range from the 10th percentile for the December-January period to the 90th percentile for May); the hypothetical value of 0.

As in the case of single-variable parameterizations, example families of $a_{ph}{}^*$ curves are now presented for the new two-component parameterization (Figure 8) for two values of $\Sigma C_i/Tchla$, i.e. 0.47 and 0.88, corresponding to the 10th and 90th percentiles from the observed distribution of that ratio. There are conspicuous differences in this respect between both the values and the shapes of the $a_{ph}{}^*$ spectra. As expected, the new two-component parameterization generally predicts lower values of $a_{ph}{}^*(\lambda)$ for lower values of $\Sigma C_i/Tchla$ than for higher ones. If we assume a low proportion of accessory pigments, i.e. for $\Sigma C_i/Tchla = 0.47$ and $Tchla$ increasing from 0.3 to 100 mg m^{-3}, the colour index falls from 2.69 to 1.72, i.e. by a factor of 1.57. In contrast, if we assume a higher proportion of accessory pigments (=0.88), the colour index decreases by the same factor (1.57), but from a higher starting value of 2.85, to 1.82. However, none of these differences are as distinct as those between the families of $a_{ph}{}^*$ curves, drawn earlier according to the one-component parameterizations obtained for particular months (see Figure 5). Generally speaking, we can expect the use of the two-component parameterization to introduce an additional 'degree of freedom' to the description of the variability of parametrized light absorption spectra. But it also seems likely that even with the new two-component parameterization it will not be possible to explain all the differences manifested

17

by the monthly one-component parameterizations. This intuitive expectation can be quantitatively checked by analysing in detail the estimation errors calculated for different variants of the parameterizations.
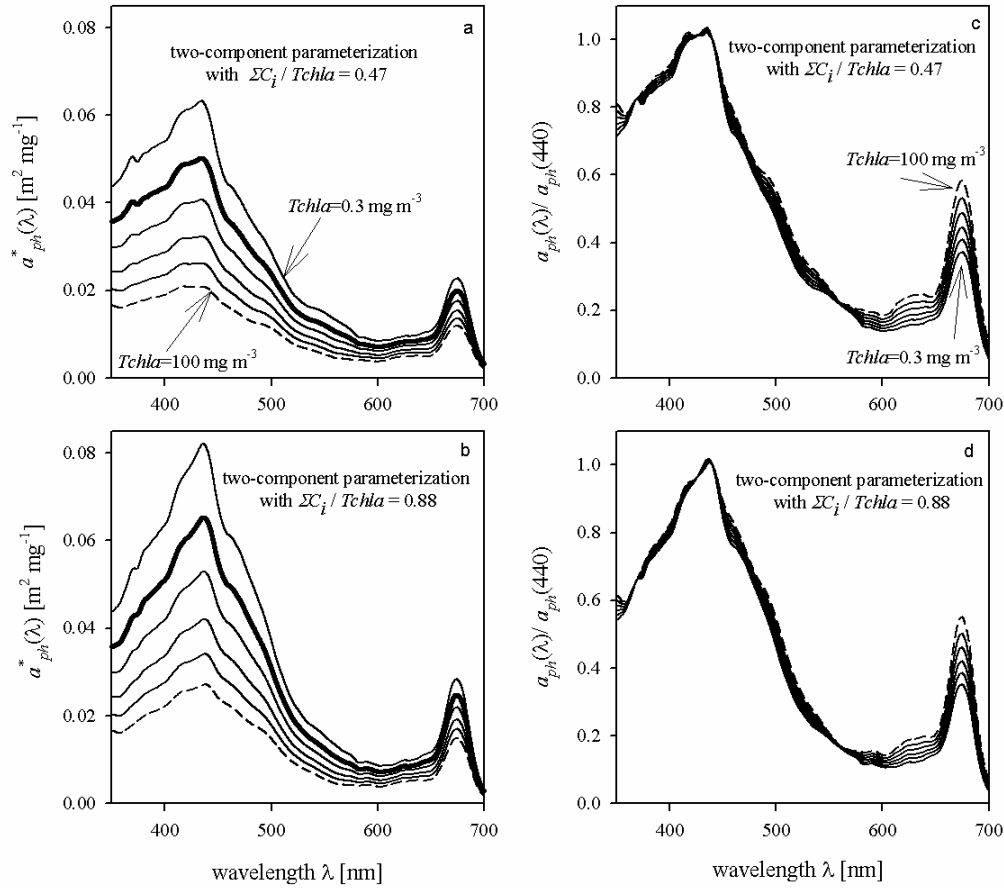
Figure 8. Example spectra of the specific coefficient of light absorption by phytoplankton a^*_{ph} (panels a and b) and spectra of coefficient a_{ph} normalized to its value in the 440 nm band (panels c and d), for some values of *Tchla* between 0.3 and 100 mg m^{-3}, estimated by the two-component parameterization Eq. (4), and for two different assumed constant values of the pigment concentration ratio $\Sigma C_i/Tchla$: 0.47 (representing the 10th percentile for all data), and 0.88 (representing the 90th percentile for all data).

3.3 Estimation errors of the different variants of parameterizations

We performed an extensive analysis of the errors arising out of the different variants of the proposed approximation formulas (analysis of estimation errors). Different cases were considered: the formulas were tested on the whole dataset as well as on data from particular months only. In our analyses we used both the arithmetic statistics of relative errors and also so-called logarithmic statistics, as these are generally appropriate when the variation of tested/estimated quantities spans several orders of magnitude. Below we present the most important results of these analyses.

18

Table 3 sets out the statistics of estimation errors when different variants of the parameterizations were tested on the whole dataset. Three scenarios were considered: first, when the general variant of the parameterization was used to calculate absorption coefficients; second, when the relevant variants of monthly parameterizations were used, depending on the month of data acquisition; and third, when the two-component parameterization was used (the values for the second and third scenarios are given in parentheses). All these results are given for nine light wavelengths chosen to cover the spectral range under consideration and include the characteristic maxima of light absorption by chlorophyll a. We found that the estimation errors of coefficients a_{ph} obtained using the general parameterization were relatively stable from 400 to 690 nm. In this range, the systematic error according to arithmetic statistics remains at the relatively low level of 5-9%, while the statistical error varies from 34% to just over 50%. Because the general parameterization was developed using linear least-squares regression applied to the logarithms of $Tchla$ and a_{ph}, the systematic error according to logarithmic statistics is always equal or very close to zero. The standard error factor x, which enables the statistical error range according to logarithmic statistics to be determined (by multiplying or dividing by its value, see formulas given as a footnote to Table 3), varies between 1.37 and 1.52 for wavelengths from 400 to 690 nm; values are higher only at the edges of the spectral range under investigation. This means that the statistical error according to logarithmic statistics in the 400-690 nm range varies from -34% to 52%; if the entire spectral range is considered, it varies from -45% to 81%. For the second scenario of calculations done over the entire dataset, i.e. when different monthly parameterization were used on an entire dataset, the errors are only slightly lower than the previous ones. Applying logarithmic statistics to this scenario leads to a standard error factor varying from 1.34 to 1.49 in the 400-690 nm range, and taking values of ≤1.75 at the edges of this range. Hence, the statistical error according to logarithmic statistics in the 400-690 nm range varies from -33% to 49%, and from -45% to 75% if the entire spectral range is considered. In the third scenario, i.e. when the new two-component parameterization was applied to a whole dataset, we found estimation errors to lie generally between the errors of the first and second scenarios. In terms of logarithmic statistics, again, as expected, the systematic errors are close to zero, and the standard error factor in the 400-690 nm range varies from 1.35 to 1.52. A detailed comparison of the results obtained indicates that applying the two-component parameterization to a whole dataset leads to a small but noticeable reduction in the errors compared with use of the general version of the one-component parameterization (Eq. 3.a) only in the 390-530 nm and 665-685 nm spectral ranges. These are the ranges in which significant differences in the family of $A'(\lambda, \Sigma C_i/Tchla)$ curves have been observed (see Figure 7b). However, comparison of the estimation errors associated with the two-component parameterization with the scenario of using monthly variants of the one-component parameterization slightly favours the latter.

Table 3. Statistics of estimation errors* of coefficient $a_{ph}(\lambda)$ in selected spectral bands when the different variants of the parameterization derived in this study were applied to the entire dataset (n= 1002). The calculated values are given for three scenarios: when the general variant of the one-component parameterization was used; when variants specific to individual months were chosen (the first alternative value is given in parentheses); and when the two-component parameterization was used (the second alternative value is given in parentheses).

λ [nm]	Arithmetic statistics of relative error			Logarithmic statistics		
	systematic error	statistical error	systematic error	standard error factor	statistical error	
	$\langle\varepsilon\rangle$ [%]	σ_ε [%]	$\langle\varepsilon\rangle_g$ [%]	x	σ_+ [%]	σ_- [%]
350	17.9 (16.0; 18.0)	68 (65; 68)	0 (-0.0; -0.1)	1.81 (1.75; 1.82)	81 (75; 82)	-45 (-43; -45)
400	8.5 (7.7; 8.1)	45 (42; 43)	0 (-0.0; -01)	1.51 (1.48; 1.51)	51 (48; 51)	-34 (-33; -34)
440	6.3 (5.2; 5.4)	39 (34; 35)	0 (-0.0; -0.1)	1.42 (1.38; 1.40)	42 (38; 40)	-30 (-28; -28)
500	6.1 (5.2; 5.2)	37 (34; 34)	0 (-0.0; -0.2)	1.42 (1.38; 1.39)	42 (38; 40)	-29 (-28; -28)
550	7.6 (6.7; 7.6)	42 (39; 43)	0 (-0.1; -0.1)	1.47 (1.44; 1.48)	48 (44; 48)	-32 (-31; -33)
600	8.8 (8.1; 8.8)	47 (46; 48)	0 (-0.2; -0.1)	1.52 (1.49; 1.52)	52 (49; 52)	-34 (-33; -34)
675	5.0 (4.2; 4.4)	34 (31; 32)	0 (-0.0; -0.2)	1.37 (1.34; 1.35)	37 (34; 36)	-27 (-25; -26)
690	5.8 (5.4; 5.8)	37 (37; 38)	0 (-0.1; -0.2)	1.40 (1.39; 1.41)	40 (39; 41)	-29 (-28; -29)
700	23.8 (21.8; 24.5)	199 (193; 194)	-0.9 (-0.2; 0.8)	1.69 (1.70; 1.74)	69 (70; 74)	-41 (-41; -42)

*) Arithmetic statistics of the relative error:
- mean of the relative error (representing the systematic error according to arithmetic statistics):

$\langle\varepsilon\rangle = N^{-1}\sum_{i=1}^{N}\varepsilon_i$, where $\varepsilon = \frac{(P_i - O_i)}{O_i}$, O_i - observed/measured values, P_i - predicted/estimated values

- the standard deviation of the relative error (representing the statistical error according to arithmetic statistics):

$\sigma_\varepsilon = \sqrt{\frac{1}{N}\left(\sum_{i=1}^{N}(\varepsilon_i - \langle\varepsilon\rangle)^2\right)}$

Logarithmic statistics:
- the mean logarithmic error (representing the systematic error according to logarithmic statistics):

$\langle\varepsilon\rangle_g = 10^{\langle\log\left(\frac{P_i}{O_i}\right)\rangle} - 1$, where $\langle\log\left(\frac{P_i}{O_i}\right)\rangle$ is the mean of $\log\left(\frac{P_i}{O_i}\right)$

- the standard error factor (the quantity which allows the range of statistical errors to be calculated according to logarithmic statistics):

$x = 10^{\sigma_{log}}$, where σ_{log} is the standard deviation of the set $\log\left(\frac{P_i}{O_i}\right)$

- statistical logarithmic errors (representing the range of statistical errors according to logarithmic statistics):

$\sigma_- = \frac{1}{x} - 1$, $\sigma_+ = x - 1$

The above estimation errors were calculated over the entire available dataset. Therefore these results do not address the question of how much more accurate the results might be if different variants of parameterization were tested on data from just one particular month. Table 4 gathers some results which address the latter question. It lists results obtained for data subsets limited to four separate months, and to light wavelengths representing only selected bands where the phytoplankton absorption is relatively high. Additionally, for brevity, only certain characteristics of the logarithmic statistics are presented. We generally found that using the monthly parameterization instead of a general variant for individual months often reduces

the level of statistical error according to both arithmetic and logarithmic statistics by only a small amount, although it may have a significant impact by strongly reducing the systematic error. Applying the general variant of the parameterization to particular months may overestimate or underestimate the values of coefficients a_{ph} by a few percent to as much as 30% and more in extreme situations (up to 25% for the spectral bands shown in Table 4). If we take the case of April, the general

5 parameterization variant overestimates $a_{ph}(\lambda)$ by ca 12% to 34%, depending on the light wavelength. For September, on the other hand, $a_{ph}(\lambda)$ is underestimated by ca 2 to 9% in the majority of the visible range. In other months $a_{ph}(\lambda)$ may be overestimated in some spectral ranges and underestimated in others. In contrast, according to expectations, using appropriately matched monthly parameterizations in all of these cases enables one to eliminate the systematic error according to logarithmic statistics and to significantly reduce the systematic error of the arithmetic statistics. Applying the two-component

10 parameterization rather than the general variant of the one-component parameterization usually leads to a reduction in the statistical errors in the vicinity of phytoplankton absorption peaks. The systematic error is reduced only in two of the months analysed (May and September), while in the others, there is no influence or even a slight increase (April and March).

Table 4. Selected characteristics of the estimation error logarithmic statistics calculated according to different parameterizations and for particular months: March, April, May and September (the numbers of data considered were 174, 96,

15 201 and 211, respectively).

Month	Variant of parameterization λ [nm]	one-component general systematic error $\langle\varepsilon\rangle_g$[%]	standard error factor x	one-component month specific systematic error $\langle\varepsilon\rangle_g$[%]	standard error factor x	two-component systematic error $\langle\varepsilon\rangle_g$[%]	standard error factor x
March							
	400	-7.4	1.56	0	1.54	-9.8	1.54
	440	1.7	1.44	0	1.42	-2.6	1.41
	500	0.8	1.45	0	1.42	-3.3	1.43
	675	-1.5	1.41	0	1.41	-4.8	1.39
April							
	400	24.9	1.46	0	1.44	25.3	1.45
	440	17.3	1.42	0	1.39	17.9	1.39
	500	13.4	1.43	0	1.38	13.9	1.38
	675	11.8	1.33	0	1.31	12.2	1.32
May							
	400	-5.7	1.47	0	1.46	-0.6	1.43
	440	-11	1.40	0	1.39	-2.6	1.34
	500	-9.8	1.39	0	1.39	-1.7	1.34
	675	-4.9	1.45	0	1.35	2.2	1.34
September							
	400	-1.7	1.41	0	1.41	-0.5	1.42
	440	-7.5	1.33	0	1.31	-5.6	1.33
	500	-4.6	1.41	0	1.31	-2.7	1.33
	675	-8.5	1.35	0	1.32	-7.0	1.34

3.4 Comparison with selected examples of parameterizations from the literature

So far, when discussing our own results, we have referred only to the 'classic' version of the parameterization given by Bricaud et al. (1995). Now we shall briefly compare our results with other examples of parameterizations from the literature. In two additional panels of Figure 5 (d and e) we have plotted the coefficients of the parameterization by Bricaud et al. (1995), as well as coefficients of four other variants obtained for different marine environments by different authors: Stramska et al. (2003), Matsuoka et al. (2007), Nima et al. (2016) and Churilova et al. (2017). These examples were chosen from among the many known in the literature, in order to illustrate the possible variability occurring between coefficients of different parameterizations that were originally matched to different datasets. In the case of coefficients *A*, all the spectral shapes presented in Figure 5d generally reflect the characteristic absorption maxima in the blue and red spectral ranges. Quantitatively, however, there are significant differences between these examples, the largest being in the wavelength range from about 400 to 480 nm. Interestingly, such a range of *A* coefficient variability resembles the one we obtained with our own Baltic data when we developed separate variants of the one-component parameterization for individual months (see Figure 5a). With regard to the values of coefficients *E*, the literature examples presented in Figure 5e differ significantly from each other and all exhibit a distinct variation of values across the spectrum. According to these literature sources, coefficients *E* can take values from less than 0.5 to even more than 1 in different spectral ranges. In our analyses we also found spectral variations of *E* values, but only for parameterization variants that were matched to the data from separate months; on pooling all our data, we found that the resulting spectral shape of coefficient *E* was relatively flat (with values between 0.8 and 0.9 for the general parameterization variant; see Figure 5b). The fact that the various literature parameterizations clearly differ in their coefficients *E* can be additionally illustrated by different slopes of curves plotted on graphs showing estimated dependences of specific absorption coefficients $a_{ph}^*(440)$ and $a_{ph}^*(675)$ as functions of *Tchla* (see Figures 6c and d). In addition to the examples mentioned earlier, we also plotted curves according to Staehr and Markager (2004) as examples representing a wide range of *Tchla*. Again, we would like to point out that the pattern of different slopes among literature examples resembles the differences we obtained from analysing the data for different months.

As a final aspect of this brief comparison, Figure 9 shows the main characteristics of the logarithmic statistics describing the accuracy of the formulas chosen from the literature when they were applied to calculate coefficient a_{ph} of our whole dataset. This was only done for illustrative purposes – in no way was it an attempt to validate our results. As may be seen from Figure 9a, all the literature formulas compared reveal significant systematic errors when they were tested on our dataset. The systematic estimation errors of $a_{ph}(\lambda)$ in the 'classic' parameterization according to Bricaud et al. (1995) range from -57 to -21% over almost the entire spectral range. Other examples show significant systematic errors at least in some portions of the light spectrum analysed (from almost -60 to about +60% at some cases). In Figure 9a we also plotted systematic errors calculated now for our own, previous preliminary version of the Baltic Sea parameterization (Meler et al. 2017a). We now see that, apart from the UV range, values of a_{ph} are generally overestimated by up to 20% and more by this earlier version of the formula. In regard to the standard error factor, we can see that only some of the literature examples in the vicinity of

phytoplankton light absorption peaks achieve similarly low values as represented by our new two-component parameterization. But since for the total estimation accuracy the contributions of both systematic and statistical errors have to be taken into account, one can expect that overall, none of the literature examples can attain the accuracy that we achieved by matching our new parameterizations to our own dataset.
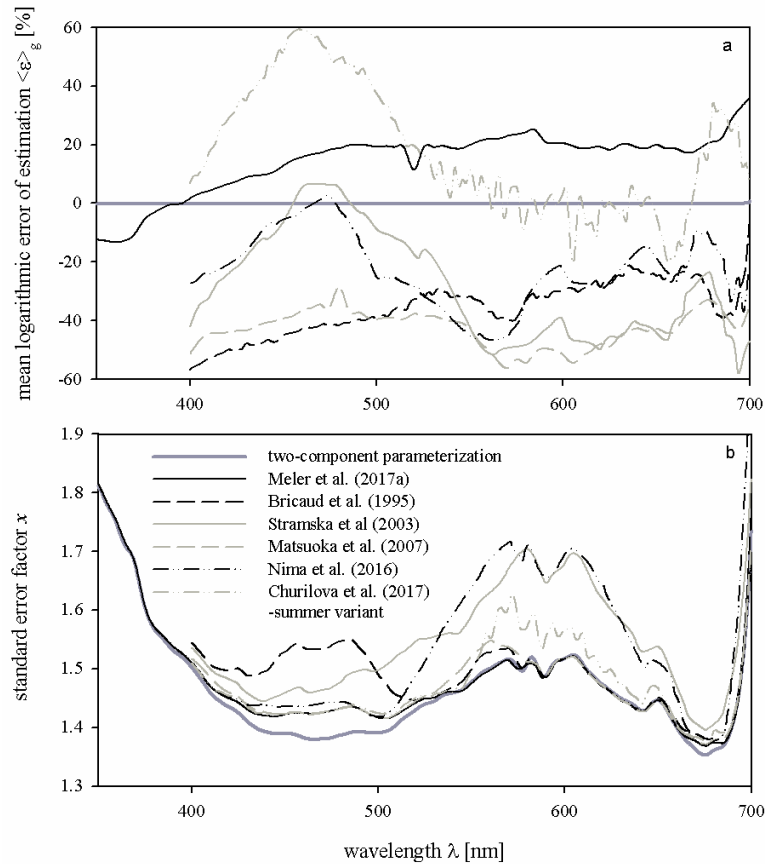
Figure 9. Comparison of the main characteristics of the estimation error logarithmic statistics calculated for various parameterizations of phytoplankton absorption coefficients: (a): the mean logarithmic errors of estimation $<\varepsilon>_g$, and (b): the standard error factor x. Different curves in these panels represent: the two-component parameterization from this study, the preliminary parameterization according to Meler et al. (2017a), and selected examples of parameterizations gleaned from the literature (according to Bricaud et al. (1995), Churilova et al. (2017), Nima et al. (2016), Matsuoka et al. (2007) and Stramska (2003)) (see the legend given in panel b). All these parameterizations were applied to our entire dataset.

4 Final remarks

The empirical material for this work was acquired in a relatively small geographical area, mainly the southern Baltic Sea. However, because it was gathered in various parts of this basin, from coastal areas to open waters, and at different times of the year, the recorded light absorption coefficients and concentrations of phytoplankton pigments have large ranges of variability, in both cases reaching almost three orders of magnitude. Based on such a dataset, it was possible to derive a number

23

of new variants of the parameterization of coefficient a_{ph}: they should be treated as simplified and practical relationships of a local character, tailored to the specifics of the target environment. The new empirical formulas include classic one-component parameterizations, where the only variable is the concentration of chlorophyll a. Parameterizations of this type have been developed both as a general version, i.e. one matched to all the data collected in different periods of the year, and in the form of separate variants adjusted to the individual months of data collection. Importantly, we found that the coefficients of monthly variants could differ from each other very significantly, thus indirectly reflecting the annual variation in the proportions between chlorophyll a and other photosynthetic or photoprotective pigments. The paper also presents a new, slightly more complex form of parameterization that uses one additional variable: the ratio of the concentrations of accessory pigments to the concentration of chlorophyll a. With all the variants of this parameterization, spectra of coefficient a_{ph} can be estimated fairly simply, and with few requirements as to input data. Such estimates can be made over a wide spectral range (from 350 to 700 nm) and with a high spectral resolution (1 nm). It should be borne in mind, however, that the accuracy of such estimates is obviously limited. For example, application of the general version of the one-component parameterization to all our data covering different periods of the year understandably leads to a practically zero systematic error of this estimate, although a significant statistical error remains. The latter may be characterized by standard error factors from 1.37 to 1.51 in the vast majority of the spectral ranges tested. However, since the real values of a_{ph} vary in Baltic Sea conditions over almost three orders of magnitude, even an estimation accuracy such as this appears satisfactory. Our study has also shown that further improvement in the accuracy of the approximate description of a_{ph} spectra is possible, at least in some applications. In the case of datasets acquired in different times of the year, such an improvement can be achieved by using either 'dynamically selected' monthly variants of parameterizations, or, when pigment composition data are available, by using the new two-component parameterization. In the case of data limited to particular months, it is possible to prevent the occurrence of significant systematic errors especially by using the appropriately selected monthly parameterization. An important qualitative observation from our analyses is that the new variants of monthly parameterizations have a range of variability of coefficients similar to that between the different literature parameterizations established on the basis of data from diverse aquatic environments. This particular observation reminds us that all such parameterizations are always quite far-reaching simplifications of relationships occurring in nature. The variability of these relationships that we recorded throughout the year in the Baltic Sea seems to indicate that only the use of a much more elaborate mathematical apparatus, using a much larger number of variables describing the composition of pigments and other features of the phytoplankton population, could further and more radically improve the accuracy of the spectral description of the light absorption coefficient (see e.g. the multi-component models presented earlier in the papers by B. Woźniak and his co-authors (Woźniak et al. 1999, Woźniak et al. 2000, Majchrowski et al. 2000, Ficek et al. 2004)). In our opinion, however, the practical value of the simple parameterizations presented in this work should be seen in the opportunities for applying them to the development of various methods and algorithms, whose specificity from the very beginning requires the use of simplifications.

24

5 Data availability

All data used in this study will be freely available, for scientific use only, upon request. Anyone interested in using this data set for scientific research should contact the corresponding author via e-mail.

Appendix 1

5   The spectral coefficients of certain variants of the parameterizations obtained in this work are given in the tables below with either 2 or 5 nm spectral steps. The values of the coefficients with 1 nm resolution and for other cases not presented below are available from the authors on request.

Table A1. Spectral coefficients A and E of the one-component parameterization described by Eq. (3.a) in its general variant (i.e. the variant obtained when all data, regardless of the month of acquisition, were taken into account) and the corresponding 10   determination coefficients R^2.

| λ [nm] | A | E | R^2 | λ [nm] | A | E | R^2 | λ [nm] | A | E | R^2 |
1	2	3	4	1	2	3	4	1	2	3	4
350	0.0358	0.833	0.69	468	0.0394	0.823	0.86	586	0.0078	0.859	0.84
352	0.0360	0.831	0.69	470	0.0387	0.822	0.86	588	0.0078	0.858	0.84
354	0.0362	0.826	0.70	472	0.0379	0.821	0.86	590	0.0078	0.859	0.84
356	0.0364	0.823	0.70	474	0.0371	0.821	0.86	592	0.0077	0.861	0.84
358	0.0368	0.820	0.70	476	0.0361	0.822	0.86	594	0.0076	0.863	0.83
360	0.0374	0.818	0.71	478	0.0353	0.823	0.86	596	0.0074	0.862	0.83
362	0.0382	0.816	0.72	480	0.0345	0.823	0.86	598	0.0073	0.861	0.83
364	0.0391	0.815	0.72	482	0.0338	0.824	0.86	600	0.0072	0.861	0.83
366	0.0401	0.814	0.73	484	0.0330	0.825	0.86	602	0.0072	0.862	0.83
368	0.0410	0.812	0.73	486	0.0323	0.827	0.86	604	0.0073	0.863	0.83
370	0.0414	0.812	0.74	488	0.0316	0.830	0.86	606	0.0073	0.864	0.83
372	0.0413	0.816	0.75	490	0.0310	0.832	0.86	608	0.0074	0.868	0.83
374	0.0413	0.820	0.77	492	0.0303	0.833	0.86	610	0.0075	0.875	0.84
376	0.0418	0.820	0.78	494	0.0295	0.835	0.86	612	0.0076	0.881	0.85
378	0.0427	0.818	0.78	496	0.0286	0.837	0.87	614	0.0077	0.885	0.85
380	0.0434	0.817	0.79	498	0.0277	0.838	0.87	616	0.0078	0.885	0.85
382	0.0437	0.818	0.79	500	0.0268	0.840	0.87	618	0.0080	0.885	0.85
384	0.0440	0.819	0.80	502	0.0257	0.842	0.87	620	0.0082	0.886	0.86
386	0.0444	0.819	0.80	504	0.0246	0.844	0.87	622	0.0083	0.887	0.86
388	0.0449	0.819	0.80	506	0.0236	0.845	0.87	624	0.0084	0.886	0.86
390	0.0451	0.818	0.80	508	0.0227	0.844	0.87	626	0.0085	0.886	0.86
392	0.0454	0.818	0.81	510	0.0217	0.844	0.87	628	0.0085	0.888	0.87
394	0.0458	0.818	0.81	512	0.0208	0.844	0.86	630	0.0085	0.889	0.87
396	0.0462	0.819	0.81	514	0.0199	0.844	0.86	632	0.0085	0.888	0.87

398	0.0465	0.819	*0.81*	**516**	0.0191	0.845	*0.86*	**634**	0.0086	0.888	*0.87*
400	0.0468	0.820	*0.82*	**518**	0.0183	0.845	*0.86*	**636**	0.0087	0.888	*0.87*
402	0.0473	0.820	*0.82*	**520**	0.0176	0.845	*0.86*	**638**	0.0088	0.887	*0.87*
404	0.0481	0.821	*0.83*	**522**	0.0170	0.845	*0.86*	**640**	0.0089	0.881	*0.87*
406	0.0491	0.820	*0.83*	**524**	0.0165	0.844	*0.86*	**642**	0.0091	0.875	*0.87*
408	0.0502	0.819	*0.83*	**526**	0.0160	0.843	*0.85*	**644**	0.0092	0.871	*0.87*
410	0.0512	0.817	*0.84*	**528**	0.0156	0.843	*0.85*	**646**	0.0093	0.869	*0.87*
412	0.0521	0.817	*0.84*	**530**	0.0151	0.843	*0.85*	**648**	0.0094	0.868	*0.86*
414	0.0528	0.817	*0.84*	**532**	0.0147	0.844	*0.85*	**650**	0.0096	0.869	*0.86*
416	0.0533	0.817	*0.84*	**534**	0.0144	0.844	*0.85*	**652**	0.0099	0.873	*0.87*
418	0.0537	0.816	*0.84*	**536**	0.0141	0.843	*0.85*	**654**	0.0104	0.877	*0.87*
420	0.0539	0.814	*0.84*	**538**	0.0139	0.841	*0.85*	**656**	0.0112	0.881	*0.88*
422	0.0541	0.814	*0.85*	**540**	0.0137	0.839	*0.85*	**658**	0.0121	0.885	*0.88*
424	0.0544	0.813	*0.85*	**542**	0.0134	0.836	*0.85*	**660**	0.0133	0.888	*0.89*
426	0.0548	0.812	*0.85*	**544**	0.0132	0.832	*0.84*	**662**	0.0148	0.889	*0.89*
428	0.0552	0.811	*0.85*	**546**	0.0129	0.829	*0.84*	**664**	0.0164	0.889	*0.89*
430	0.0556	0.810	*0.85*	**548**	0.0126	0.827	*0.84*	**666**	0.0181	0.888	*0.90*
432	0.0561	0.809	*0.85*	**550**	0.0123	0.825	*0.84*	**668**	0.0197	0.887	*0.90*
434	0.0565	0.809	*0.86*	**552**	0.0120	0.823	*0.83*	**670**	0.0208	0.888	*0.90*
436	0.0565	0.809	*0.86*	**554**	0.0116	0.821	*0.83*	**672**	0.0216	0.889	*0.90*
438	0.0561	0.810	*0.86*	**556**	0.0113	0.819	*0.83*	**674**	0.0220	0.889	*0.90*
440	0.0553	0.812	*0.86*	**558**	0.0110	0.817	*0.82*	**675**	0.0220	0.889	*0.90*
442	0.0541	0.813	*0.86*	**560**	0.0107	0.816	*0.82*	**676**	0.0219	0.889	*0.90*
444	0.0525	0.815	*0.86*	**562**	0.0105	0.816	*0.82*	**678**	0.0214	0.889	*0.90*
446	0.0506	0.817	*0.86*	**564**	0.0102	0.819	*0.82*	**680**	0.0204	0.889	*0.90*
448	0.0486	0.819	*0.86*	**566**	0.0100	0.822	*0.82*	**682**	0.0190	0.890	*0.90*
450	0.0469	0.821	*0.86*	**568**	0.0098	0.824	*0.82*	**684**	0.0170	0.894	*0.90*
452	0.0453	0.824	*0.86*	**570**	0.0096	0.826	*0.82*	**686**	0.0146	0.898	*0.90*
454	0.0440	0.826	*0.86*	**572**	0.0094	0.827	*0.82*	**688**	0.0121	0.902	*0.90*
456	0.0429	0.827	*0.86*	**574**	0.0091	0.831	*0.82*	**690**	0.0098	0.904	*0.89*
458	0.0421	0.828	*0.86*	**576**	0.0089	0.836	*0.83*	**692**	0.0079	0.905	*0.88*
460	0.0416	0.827	*0.86*	**578**	0.0086	0.843	*0.83*	**694**	0.0062	0.906	*0.86*
462	0.0412	0.825	*0.86*	**580**	0.0082	0.851	*0.83*	**696**	0.0049	0.909	*0.84*
464	0.0407	0.824	*0.86*	**582**	0.0079	0.857	*0.83*	**698**	0.0039	0.912	*0.81*
466	0.0401	0.823	*0.86*	**584**	0.0078	0.859	*0.83*	**700**	0.0031	0.913	*0.76*

Table A2. Spectral coefficients *A* and *E* of the one-component parameterization described by Eq. (3.a) in its variants obtained in selected months and the corresponding determination coefficients R^2.

λ [nm]	March			April			May			September		
1	*A*	*E*	R^2	*A*	*E*	R^2	*A*	*E*	R^2	*A*	*E*	R^2
	2	*3*	*4*	*2*	*3*	*4*	*2*	*3*	*4*	*2*	*3*	*4*
350	0.0368	0.971	*0.75*	0.0312	0.816	*0.77*	0.0352	0.876	*0.82*	0.0273	0.911	*0.74*
355	0.0371	0.961	*0.75*	0.0298	0.826	*0.78*	0.0352	0.866	*0.83*	0.0285	0.902	*0.75*
360	0.0371	0.959	*0.75*	0.0302	0.814	*0.77*	0.0364	0.865	*0.83*	0.0311	0.874	*0.75*
365	0.0384	0.946	*0.75*	0.0309	0.826	*0.78*	0.0382	0.865	*0.83*	0.0354	0.846	*0.75*
370	0.0396	0.945	*0.77*	0.0318	0.823	*0.77*	0.0399	0.866	*0.84*	0.0384	0.836	*0.77*
375	0.0395	0.950	*0.81*	0.0292	0.869	*0.82*	0.0412	0.865	*0.86*	0.0395	0.833	*0.82*
380	0.0412	0.943	*0.82*	0.0297	0.880	*0.84*	0.0441	0.853	*0.86*	0.0429	0.815	*0.82*
385	0.0417	0.945	*0.83*	0.0302	0.885	*0.85*	0.0452	0.853	*0.87*	0.0451	0.803	*0.83*
390	0.0421	0.943	*0.83*	0.0309	0.886	*0.85*	0.0462	0.851	*0.88*	0.0472	0.792	*0.83*
395	0.0430	0.936	*0.83*	0.0315	0.890	*0.85*	0.0469	0.853	*0.88*	0.0495	0.784	*0.83*
400	0.0439	0.935	*0.84*	0.0311	0.903	*0.86*	0.0471	0.858	*0.89*	0.0514	0.777	*0.84*
405	0.0452	0.934	*0.85*	0.0318	0.916	*0.87*	0.0487	0.858	*0.89*	0.0548	0.766	*0.85*
410	0.0476	0.921	*0.85*	0.0333	0.920	*0.87*	0.0519	0.854	*0.89*	0.0589	0.756	*0.86*
415	0.0489	0.914	*0.86*	0.0346	0.923	*0.88*	0.0541	0.852	*0.90*	0.0624	0.750	*0.86*
420	0.0496	0.905	*0.86*	0.0350	0.927	*0.87*	0.0554	0.847	*0.90*	0.0642	0.745	*0.87*
425	0.0499	0.898	*0.87*	0.0353	0.931	*0.88*	0.0569	0.842	*0.90*	0.0658	0.737	*0.87*
430	0.0504	0.893	*0.87*	0.0354	0.936	*0.89*	0.0586	0.837	*0.90*	0.0681	0.728	*0.87*
435	0.0508	0.889	*0.87*	0.0356	0.942	*0.89*	0.0608	0.832	*0.90*	0.0703	0.721	*0.88*
440	0.0493	0.892	*0.88*	0.0351	0.945	*0.89*	0.0602	0.835	*0.90*	0.0698	0.718	*0.88*
445	0.0458	0.900	*0.88*	0.0329	0.951	*0.89*	0.0568	0.834	*0.90*	0.0648	0.720	*0.88*
450	0.0417	0.912	*0.88*	0.0300	0.959	*0.89*	0.0514	0.841	*0.90*	0.0585	0.722	*0.88*
455	0.0386	0.921	*0.88*	0.0282	0.965	*0.89*	0.0481	0.844	*0.90*	0.0543	0.719	*0.89*
460	0.0366	0.926	*0.88*	0.0268	0.973	*0.90*	0.0464	0.841	*0.90*	0.0525	0.712	*0.89*
465	0.0354	0.918	*0.88*	0.0259	0.974	*0.90*	0.0449	0.839	*0.90*	0.0516	0.705	*0.89*
470	0.0338	0.913	*0.88*	0.0242	0.980	*0.90*	0.0428	0.840	*0.89*	0.0501	0.698	*0.89*
475	0.0318	0.911	*0.88*	0.0226	0.979	*0.89*	0.0405	0.839	*0.89*	0.0474	0.702	*0.89*
480	0.0356	0.915	*0.88*	0.0211	0.979	*0.89*	0.0382	0.842	*0.89*	0.0448	0.705	*0.89*
485	0.0281	0.920	*0.88*	0.0196	0.988	*0.89*	0.0364	0.843	*0.89*	0.0423	0.708	*0.89*
490	0.0266	0.930	*0.88*	0.0188	0.990	*0.90*	0.0346	0.844	*0.90*	0.0399	0.715	*0.89*
495	0.0250	0.939	*0.89*	0.0178	0.996	*0.90*	0.0323	0.845	*0.90*	0.0370	0.722	*0.89*
500	0.0233	0.945	*0.89*	0.0166	0.998	*0.91*	0.0291	0.853	*0.91*	0.0336	0.727	*0.88*
505	0.0213	0.950	*0.89*	0.0150	0.999	*0.91*	0.0255	0.862	*0.91*	0.0299	0.734	*0.88*
510	0.0193	0.952	*0.88*	0.0139	0.989	*0.90*	0.0230	0.859	*0.91*	0.0263	0.741	*0.87*
515	0.0173	0.960	*0.88*	0.0124	0.992	*0.90*	0.0203	0.862	*0.91*	0.0233	0.744	*0.87*
520	0.0157	0.964	*0.88*	0.0109	1.000	*0.90*	0.0179	0.864	*0.90*	0.0207	0.748	*0.86*
525	0.0147	0.958	*0.88*	0.0101	0.999	*0.90*	0.0162	0.864	*0.90*	0.0192	0.744	*0.86*

530	0.0139	0.953	*0.88*	0.0092	1.005	*0.89*	0.0148	0.867	*0.90*	0.0180	0.746	*0.86*
535	0.0132	0.953	*0.87*	0.0086	1.008	*0.90*	0.0133	0.881	*0.90*	0.0173	0.738	*0.85*
540	0.0128	0.939	*0.87*	0.0080	1.015	*0.89*	0.0125	0.881	*0.90*	0.0168	0.729	*0.85*
545	0.0121	0.934	*0.87*	0.0076	1.006	*0.89*	0.0116	0.875	*0.90*	0.0163	0.721	*0.84*
550	0.0113	0.931	*0.87*	0.0070	1.001	*0.88*	0.0106	0.878	*0.90*	0.0156	0.713	*0.83*
555	0.0106	0.917	*0.86*	0.0067	0.983	*0.88*	0.0097	0.872	*0.89*	0.0144	0.719	*0.82*
560	0.0123	0.911	*0.87*	0.0061	0.970	*0.87*	0.0090	0.873	*0.89*	0.0134	0.728	*0.82*
565	0.0092	0.910	*0.85*	0.0059	0.953	*0.87*	0.0081	0.892	*0.88*	0.0126	0.738	*0.82*
570	0.0089	0.903	*0.85*	0.0059	0.929	*0.87*	0.0075	0.906	*0.88*	0.0117	0.763	*0.82*
575	0.0084	0.912	*0.85*	0.0059	0.915	*0.87*	0.0074	0.904	*0.89*	0.0104	0.796	*0.83*
580	0.0081	0.911	*0.84*	0.0055	0.925	*0.89*	0.0065	0.934	*0.87*	0.0088	0.837	*0.84*
585	0.0077	0.930	*0.85*	0.0056	0.912	*0.88*	0.0068	0.908	*0.89*	0.0078	0.874	*0.85*
590	0.0076	0.931	*0.85*	0.0055	0.911	*0.88*	0.0071	0.902	*0.89*	0.0080	0.867	*0.86*
595	0.0074	0.925	*0.84*	0.0053	0.907	*0.88*	0.0066	0.916	*0.88*	0.0077	0.873	*0.85*
600	0.0073	0.913	*0.83*	0.0055	0.872	*0.85*	0.0060	0.933	*0.89*	0.0075	0.881	*0.85*
605	0.0074	0.910	*0.83*	0.0056	0.863	*0.86*	0.0059	0.946	*0.89*	0.0076	0.883	*0.84*
610	0.0075	0.920	*0.84*	0.0060	0.864	*0.87*	0.0063	0.942	*0.89*	0.0076	0.899	*0.84*
615	0.0078	0.935	*0.85*	0.0061	0.882	*0.87*	0.0063	0.971	*0.87*	0.0080	0.902	*0.86*
620	0.0081	0.941	*0.86*	0.0062	0.906	*0.87*	0.0071	0.943	*0.90*	0.0086	0.893	*0.86*
625	0.0084	0.933	*0.87*	0.0067	0.907	*0.89*	0.0076	0.928	*0.90*	0.0090	0.886	*0.86*
630	0.0085	0.931	*0.86*	0.0071	0.893	*0.89*	0.0072	0.948	*0.91*	0.0091	0.883	*0.86*
635	0.0086	0.935	*0.87*	0.0071	0.897	*0.90*	0.0074	0.950	*0.91*	0.0093	0.878	*0.87*
640	0.0084	0.921	*0.87*	0.0073	0.894	*0.90*	0.0078	0.944	*0.91*	0.0099	0.861	*0.86*
645	0.0090	0.895	*0.86*	0.0072	0.895	*0.90*	0.0080	0.935	*0.91*	0.0106	0.848	*0.86*
650	0.0093	0.899	*0.85*	0.0072	0.903	*0.89*	0.0081	0.948	*0.90*	0.0116	0.830	*0.85*
655	0.0106	0.907	*0.86*	0.0082	0.915	*0.90*	0.0093	0.951	*0.91*	0.0130	0.831	*0.87*
660	0.0129	0.932	*0.88*	0.0101	0.934	*0.91*	0.0123	0.946	*0.92*	0.0161	0.829	*0.88*
665	0.0168	0.933	*0.88*	0.0130	0.954	*0.92*	0.0165	0.942	*0.93*	0.0215	0.809	*0.89*
670	0.0200	0.938	*0.89*	0.0155	0.966	*0.92*	0.0208	0.929	*0.93*	0.0266	0.791	*0.89*
675	0.0211	0.937	*0.89*	0.0164	0.970	*0.93*	0.0220	0.927	*0.94*	0.0284	0.787	*0.89*
680	0.0195	0.928	*0.89*	0.0152	0.966	*0.93*	0.0201	0.933	*0.94*	0.0265	0.789	*0.89*
685	0.0153	0.926	*0.89*	0.0120	0.954	*0.92*	0.0153	0.944	*0.94*	0.0196	0.817	*0.88*
690	0.0096	0.938	*0.89*	0.0077	0.932	*0.91*	0.0089	0.967	*0.93*	0.0112	0.862	*0.86*
695	0.0055	0.956	*0.86*	0.0045	0.908	*0.89*	0.0047	0.981	*0.90*	0.0057	0.899	*0.82*
700	0.0031	0.979	*0.81*	0.0023	0.906	*0.82*	0.0022	1.030	*0.81*	0.0029	0.938	*0.72*

Table A3. Spectral coefficients A_0 and K of the two-component parameterization described by Eq. (4). The other coefficient E is the same as in the case of the one-component parameterization (see Table A1).

| λ [nm] | A_0 | K | λ [nm] | A_0 | K | λ [nm] | A_0 | K |
1	2	3	1	2	3	1	2	3
350	0.0356	-0.007	468	0.0228	-0.831	586	0.0075	-0.053
352	0.0358	-0.007	470	0.0223	-0.836	588	0.0074	-0.094
354	0.0361	-0.005	472	0.0218	-0.840	590	0.0072	-0.127
356	0.0363	-0.007	474	0.0213	-0.842	592	0.0070	-0.139
358	0.0364	-0.018	476	0.0208	-0.843	594	0.0070	-0.130
360	0.0365	-0.038	478	0.0203	-0.842	596	0.0069	-0.112
362	0.0368	-0.058	480	0.0199	-0.840	598	0.0069	-0.093
364	0.0371	-0.077	482	0.0195	-0.838	600	0.0069	-0.063
366	0.0376	-0.095	484	0.0191	-0.833	602	0.0071	-0.034
368	0.0379	-0.119	486	0.0188	-0.822	604	0.0072	-0.018
370	0.0375	-0.151	488	0.0186	-0.805	606	0.0072	-0.019
372	0.0367	-0.181	490	0.0185	-0.782	608	0.0073	-0.020
374	0.0361	-0.204	492	0.0184	-0.758	610	0.0074	-0.014
376	0.0360	-0.228	494	0.0182	-0.734	612	0.0076	0.000
378	0.0361	-0.257	496	0.0180	-0.706	614	0.0078	0.017
380	0.0360	-0.285	498	0.0178	-0.675	616	0.0079	0.020
382	0.0358	-0.303	500	0.0175	-0.643	618	0.0080	-0.004
384	0.0359	-0.309	502	0.0172	-0.614	620	0.0079	-0.045
386	0.0362	-0.314	504	0.0167	-0.587	622	0.0079	-0.080
388	0.0363	-0.323	506	0.0163	-0.564	624	0.0080	-0.083
390	0.0362	-0.334	508	0.0158	-0.546	626	0.0081	-0.071
392	0.0362	-0.345	510	0.0153	-0.530	628	0.0081	-0.061
394	0.0362	-0.359	512	0.0149	-0.512	630	0.0081	-0.066
396	0.0362	-0.372	514	0.0144	-0.494	632	0.0081	-0.082
398	0.0362	-0.384	516	0.0139	-0.477	634	0.0081	-0.096
400	0.0361	-0.395	518	0.0135	-0.465	636	0.0081	-0.109
402	0.0362	-0.408	520	0.0130	-0.455	638	0.0081	-0.121
404	0.0364	-0.423	522	0.0127	-0.443	640	0.0081	-0.144
406	0.0369	-0.435	524	0.0124	-0.428	642	0.0082	-0.167
408	0.0374	-0.447	526	0.0122	-0.411	644	0.0081	-0.190
410	0.0378	-0.460	528	0.0121	-0.389	646	0.0081	-0.202
412	0.0382	-0.472	530	0.0119	-0.361	648	0.0082	-0.209
414	0.0384	-0.483	532	0.0118	-0.333	650	0.0084	-0.209
416	0.0385	-0.493	534	0.0118	-0.306	652	0.0087	-0.202
418	0.0385	-0.504	536	0.0117	-0.281	654	0.0091	-0.207
420	0.0384	-0.518	538	0.0118	-0.254	656	0.0096	-0.231
422	0.0382	-0.533	540	0.0118	-0.227	658	0.0102	-0.265

424	0.0380	-0.548	**542**	0.0118	-0.200	**660**	0.0109	-0.299
426	0.0378	-0.563	**544**	0.0118	-0.172	**662**	0.0119	-0.330
428	0.0377	-0.580	**546**	0.0117	-0.143	**664**	0.0129	-0.372
430	0.0376	-0.596	**548**	0.0117	-0.114	**666**	0.0137	-0.428
432	0.0376	-0.610	**550**	0.0116	-0.087	**668**	0.0143	-0.485
434	0.0374	-0.627	**552**	0.0114	-0.069	**670**	0.0148	-0.524
436	0.0370	-0.646	**554**	0.0112	-0.055	**672**	0.0152	-0.542
438	0.0363	-0.664	**556**	0.0110	-0.041	**674**	0.0154	-0.542
440	0.0355	-0.677	**558**	0.0108	-0.027	**675**	0.0155	-0.537
442	0.0345	-0.686	**560**	0.0106	-0.015	**676**	0.0155	-0.531
444	0.0333	-0.695	**562**	0.0105	0.000	**678**	0.0152	-0.515
446	0.0319	-0.702	**564**	0.0103	0.019	**680**	0.0148	-0.491
448	0.0305	-0.710	**566**	0.0102	0.039	**682**	0.0141	-0.453
450	0.0292	-0.721	**568**	0.0101	0.052	**684**	0.0131	-0.393
452	0.0279	-0.736	**570**	0.0099	0.050	**686**	0.0119	-0.310
454	0.0268	-0.754	**572**	0.0095	0.025	**688**	0.0105	-0.217
456	0.0258	-0.774	**574**	0.0091	-0.006	**690**	0.0090	-0.132
458	0.0250	-0.791	**576**	0.0088	-0.021	**692**	0.0076	-0.054
460	0.0245	-0.804	**578**	0.0085	-0.007	**694**	0.0064	0.042
462	0.0242	-0.811	**580**	0.0082	0.014	**696**	0.0054	0.157
464	0.0238	-0.817	**582**	0.0079	0.012	**698**	0.0046	0.260
466	0.0233	-0.825	**584**	0.0077	-0.014	**700**	0.0038	0.306

Appendix 2

In order to derive the two-component parameterization, the relationship described earlier by formula (3.a) was treated as a first, intermediate stage in its construction (see the examples plotted at two wavelengths in Figures A1a and b). To distinguish between them, the values calculated according to formula (3.a) are now denoted $a_{ph}(\lambda)_{cal}$, whereas the actually measured values of the absorption coefficient are $a_{ph}(\lambda)_m$. In the next step, the relationship between the ratio $a_{ph}(\lambda)_{cal}/a_{ph}(\lambda)_m$ and the ratio of the sum of accessory pigments to the concentration of chlorophyll a $\Sigma C_i/Tchla$ was analysed. Figures A1c and d illustrate the frequency distributions of the ratio $a_{ph}(\lambda)_{cal}/a_{ph}(\lambda)_m$, while Figures A1e and f show the relationships between the ratios $a_{ph}(\lambda)_m/a_{ph}(\lambda)_{cal}$ and $\Sigma C_i/Tchla$. Despite the large dispersion of individual data points on the latter two panels, the general tendency for the logarithm of $a_{ph}(\lambda)_m/a_{ph}(\lambda)_{cal}$ to decrease with increasing $\Sigma C_i/Tchla$ is evident. This tendency can be approximated by a linear function, which effectively allows one to establish coefficients of an approximate exponential relationship between the two ratios investigated:

$$\frac{a_{ph}(\lambda)_{cal}}{a_{ph}(\lambda)_m} = f\left(\frac{\Sigma C_i}{Tchla}\right) = const_1(\lambda)e^{const_2(\lambda)\frac{\Sigma C_i}{Tchla}}. \tag{A.1}$$

Relationships of this form were determined over the entire spectral range (350-700 nm) with a step of 1 nm. Obviously, the determination coefficients R^2 of the approximations are low, but this procedure generally permits additional information on the influence of pigment composition on the ultimate values of a_{ph} to be taken into account. Having the statistical dependences described by first stage formulas (3.a) and second stage formulas (A.1) to hand, a new expression can be written that approximates $a_{ph}(\lambda)$ by treating it as a function of two variables at each light wavelength – chlorophyll a concentration (*Tchla* [mg m^{-3}]) and the ratio of the sum of the concentrations of the other accessory pigments to chlorophyll a ($\Sigma C_i/Tchla$):

$$a_{ph}(\lambda) = A_0(\lambda) \cdot e^{K(\lambda)\cdot\frac{\Sigma C_i}{Tchla}} \cdot Tchla^{E(\lambda)}. \tag{A.2}$$

The numerical coefficients of the newly obtained parameterization, i.e. $A_0(\lambda)$ [m^2 mg^{-1}] (where $A_0(\lambda)=A(\lambda)/const_1(\lambda)$) and $K(\lambda)$ [no units] (where $K(\lambda)=-const_2(\lambda)$), are summarized in Table A3 in Appendix 1. Coefficient $E(\lambda)$ [no units] takes the same values as those in the general variant of the one-component parameterization.
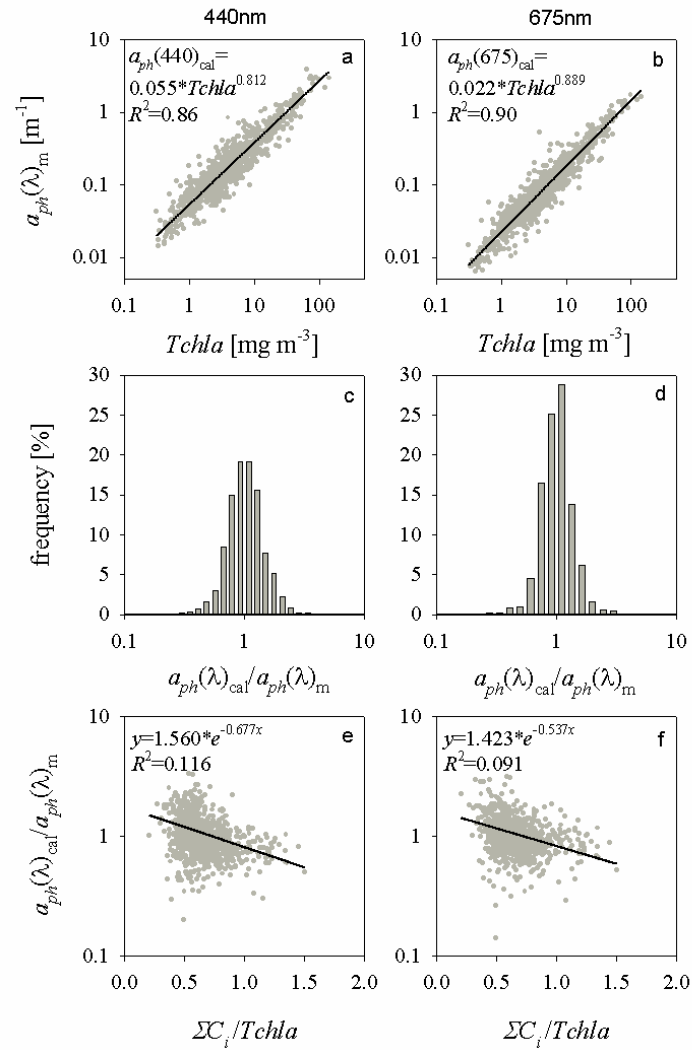
Figure A1. (a) and (b): Relations between measured coefficients of absorption by phytoplankton (denoted by $a_{ph}(\lambda)_m$) and chlorophyll *a* concentrations for two light wavelengths, 400 and 675 nm, and their functional approximations according to Eq. (3.a) (the equations are given in the panels); (c) and (d): frequency distribution histograms of the ratio of calculated and measured absorption coefficients ($a_{ph}(\lambda)_{cal}/a_{ph}(\lambda)_m$); (e) and (f): relations between the ratio $a_{ph}(\lambda)_{cal}/a_{ph}(\lambda)_m$ and the pigment concentration ratio $\Sigma C_i/Tchla$, and their functional approximations (the equations are given in the panels).

References

Babin, M., and Stramski, D., 2002. Light absorption by aquatic particles in the near-infrared spectral region. Limnol. Oceanogr. 47(3), 911-915.

Babin, M., Stramski, D., Ferrari, G. M., Claustre, H., Bricaud, A., Obolensky, G., Hoepffner, N., 2003. Variations in the light absorption coefficient of phytoplankton, nonalgal particles, and dissolved organic matter in coastal waters around Europe. J. Geophys. Res. 108(C8):3211.

Bricaud, A., Babin, M., Morel, A., Claustre, H., 1995. Variability in the chlorophyll-specific absorption coefficients of natural phytoplankton: Analysis and parameterization. J. Geophys. Res. 100:13321–13332.

Bricaud, A., Morel, A., Babin, M., Allali, K., Claustre, H., 1998. Variations of light absorption by suspended particles with chlorophyll a concentration in oceanic (case 1) waters: analysis and implications for bio-optical models. J. Geophys. Res. 103:31033-31044.

Bricaud, A., Claustre, H., Ras, J., Oubelkheir, K., 2004. Natural variability of phytoplankton absorption in oceanic waters: influence of the size structure of algal populations. Journal of Geophysical Research, 109, C11010.

Churilova, T., Suslin, V., Krivenko, O., Efimova, T., Moiseeva, N., Mukhanov, V., Smirnova, L., 2017. Light Absorption by Phytoplankton in the Upper Mixed Layer of the Black Sea: Seasonality and Parameterization. Front. Mar. Sci. 4:90. doi:10.3389/fmars.2017.00090

Dmitriev, E.V., Khomenko, G., Chami, M., Sokolov, A.A., Churilova, T., Korotaev, G. K., 2009. Parameterization of light absorption by components of seawater in optically complex coastal waters of the Crimea Penisula (Black Sea). Applied Optics 48(7), 1249-1261.

Ficek, D., Meler, J., Zapadka, T., Stoń-Egiert, J., 2012b. Modelling the light absorption coefficients of phytoplankton in Pomeranian lakes (Northern Poland), Fund. Appl. Hydrophysics, 5(4), 54-63.

Ficek, D., Meler, J., Zapadka, T., Woźniak, B., Dera, J., 2012 a. Inherent optical properties and remote sensing reflectance of Pomeranian lakes (Poland), Oceanologia, 54(4), 611-630.

Ficek, D., Kaczmarek, S., Stoń-Egiert, J., Woźniak, B., Majchrowski, R., Dera, J., 2004. Spectra of Light absorption by phytoplankton pigments In the Baltic; conclusions to be drawn from a Gaussian analysis of empirical data, Oceanologia, 46(4), 533-555.

Kirk, J.T.O., 1994. Light and Photosynthesis in Aquatic Ecosystems, Cambridge University Press, London-New York, 509.

Koblentz-Mishke, O.I., Woźniak, B., Kaczmarek, S., Konovalov, B.V.,1995. The assimilation of light energy by marine phytoplankton. Part 1. The light absorption capacity of the Baltic and Black Sea phytoplankton (methods; relation to chlorophyll concentration), Oceanologia, 37(2), 145-169.

Majchrowski, R., Woźniak, B., Dera, J., Ficek, D., Kaczmarek, S., Ostrowska, M., Koblentz-Mishke, O.I., 2000. Model of the in vivo spectral absorption of algal pigments. Part 2. Practical applications of the model. Oceanologia, 42 (2), 191-202.

Matusoka, A., Hout, Y., Shimada, K., Saitoh, S., Babin, M., 2007. Bio-optical characteristics of the western Artic Ocean: implications for ocean color algorithms. Can. J. Remote Sensing. 33(6), 503-518.

Meler, J., Ostrowska, M., Stoń-Egiert, J., 2016b. Seasonal and spatial variability of phytoplankton and non-algal absorption in the surface layer of the Baltic. Estuar. Coast. Shelf S., 180:123-135, doi: 10.1016/j.ecss.2016.06.012.

Meler, J., Kowalczuk, P., Ostrowska, M., Ficek, D., Zabłocka, M., Zdun, A., 2016a. Parameterization of the light absorption properties of chromophoric dissolved organic matter in the Baltic Sea and Pomeranian Lakes. Ocean Sciences, 12, 1013-1032, doi:10.5194/os-12-1013-2016.

Meler, J., Ostrowska, M., Ficek, D., Zdun, A., 2017a. Light absorption by phytoplankton in the southern Baltic and Pomeranian lakes: mathematical expressions for remote sensing applications. Oceanologia 59 (2017) 195-212, http://dx.doi.org/10.1016/j.oceano.2017.03.010

Meler, J., Ostrowska, M., Stoń-Egiert, J., Zabłocka, M., 2017b. Seasonal and spatial variability of light absorption by suspended particles in the southern Baltic: a mathematical description. Journal of Marine Systems 170 (2017) 68–87, http://dx.doi.org/10.1016/j.jmarsys.2016.10.011

Mitchell, B.G., 1990. Algorithm for determining the absorption coefficient of aquatic particulates using the quantitative filter technique. Proceedings of SPIE. 1302:137-148.

Mitchell, B.G., Kahru, M., Wieland, J., Stramska, M., 2002. Determination of spectral absorption coefficients of particles, dissolved material and phytoplankton for discrete water samples, in: Fargion, G.S., Mueller, J.L., [eds.] Ocean Optics

Protocols For Satellite Ocean Color Sensor Validation, Revision 3,Vol. 2, NASA Technical Memorandum 2002-210004/Rev 3-Vol 2,Chapter 15, p. 231-257.

Mobley, B. D., Light and Water, 1994. Radiative Transfer in Natural Waters, Acad. Press, San Diego, pp. 592.

Morel, A., Bricaud, A., 1981. Theoretical results concerning light absorption in a discrete medium, and application to specific absorption of phytoplankton. Deep-Sea Res. 28(11):1375–1393, 10.1016/0198-0149(81)90039-X.

Morel, A., Bricaud, A., 1986. Inherent optical properties of algal cells including picoplankton: theoretical and experimental results, in Photosynthetic picoplankton, T. Platt and W. K. W. Li, editors, Can. Bull. Fish. Aquat. Sci. 214, 521-559.

Nima, C., Frette, Ø., Hamre, B., Erga, S., Chen, Y., Zhao, L., Sørensen, K., Norli, M., Stamnes, K., Stamnes, J., 2016. Absorption properties of high-latitude Norwegian coastal water: The impact of CDOM and particulate matter. Estuar. Coast. Shelf S. 178, 158-167, 10.1016/j.ecss.2016.05.012.

Paavel, B., Kangro, K., Arst, H., Reinart, A., Kutser, T., Noges, T., 2016. Parameterization of chlorophyll-specific phytoplankton absorption coefficients for productive lake waters, J. Limnol., 75(3), 423-438.

Staehr, P.A., Markager, S., 2004. Parameterization of the chlorophyll a-specific in vivo light absorption coefficient covering estuarine, coastal and oceanic waters. Int. J. Remote Sens. 25(22):5117-5130.

Stoń, J., Kosakowska, A., 2002. Phytoplankton pigments designation – an application of RP-HPLC in qualitative and quantitative analysis. J. Appl. Phycol. 14:205-210.

Stoń-Egiert, J., Kosakowska, A., 2005. RP-HPLC determination of phytoplankton pigments comparison of calibration results for two columns. Mar. Bio. 147:251-260.

Stramska, M., Stramski, D., Hapter, R., Kaczmarek, S., Stoń, J.. 2003. Bio-optical 712 relationships and ocean color algorithms for the north polar region of the Atlantic. J. 713 Geophys. Res. 108(C5):3143, doi:10.1029/2001JC001195.

Stramski, D., Reynolds R.I., Kaczmarek, S., Uitz, J., Zheng, G., 2015. Correction of pathlength amplification in the filter-pad technique for measurements of particulate absorption coefficient in the visible spectral region. Applied Optics 54(22):6763-6782.

Tassan, S., Ferrari, G.M., 1995. An Alternative Approach to Absorption Measurements of Aquatic Particles Retained on Filters. Limnol. Oceanogr. 40(8):1358-1368.

Tassan, S., Ferrari, G.M., 2002. A sensitivity analysis of the 'Transmittance-Reflectance' method for measuring light absorption by aquatic particles. J. Plankton Res. 24(8):757–774, doi:10.1093/plankt/24.8.757.

Woźniak, B., Ostrowska, M., 1990a. Composition and resources of photosynthetic pigments of the sea phytoplankton, Oceanologia, 29, 91-115.

Woźniak, B., Ostrowska, M., 1990b. Optical absorption properties of phytoplankton in various seas, Oceanologia, 29, 147-174.

Woźniak, B., Dera, J.,2007. Light Absorption in Sea Water. Springer., New York.

Woźniak, B., Dera, J., Ficek, D., Majchrowski, R., Kaczmarek, S., Ostrowska, M., Koblentz-Mishke, O.I., 1999. Modelling the influence of acclimation on the absorption properties of marine phytoplankton. Oceanologia. 41(2):187-210.

Woźniak, B., Dera, J., Ficek, D., Majchrowski, R., Kaczmarek, S., Ostrowska, M., Koblentz-Mishke, O.I., 2000. Model of the 'in vivo' spectral absorption of algal pigments. Part 1. Mathematical apparatus, Oceanologia, 42(2), 177–190.

Woźniak, B., Dera, J., Ficek, D., Majchrowski, R., Kaczmarek, S., Ostrowska, M., Koblentz-Mishke, O.I., 2000. Model of the 'in vivo' spectral absorption of algal pigments. Part 2. Practical applications of the model. Oceanologia. 42(2):191-202.

Woźniak, S.B., Meler, J., Lednicka, B., Zdun, A., Stoń-Egiert, J., 2011a. Inherent optical properties of suspended particulate matter in the southern Baltic Sea. Oceanologia. 53(3):691-729.

Ylöstalo, P., Kallio, K., Seppälä, J., 2014. Absorption properties of in-water constituents and their variation among various lake types in the boreal region. Remote Sens. Environ. 148:190-205.

Acknowledgements

5

The authors declare that they have no conflict of interest.